Chloride-salinity as indicator of the chemical composition of groundwater: empirical predictive model based on aquifers in Southern Quebec, Canada

Lamine Boumaiza[1,2], Julien Walter[1,2], Romain Chesnaux[1,2], Randy L. Stotler[3], Tao Wen[4], Karen H. Johannesson[5], Karthikeyan Brindha[6], Frédéric Huneau[7,8]

[1] Département des Sciences appliquées, Université du Québec à Chicoutimi, Saguenay, QC, G7H 2B1, Canada

[2] Centre d'études sur les ressources minérales, Groupe de recherche Risque Ressource Eau, Université du Québec à Chicoutimi, Saguenay, QC, G7H 2B1, Canada

[3] Department of Earth and Environmental Sciences, University of Waterloo, Waterloo, ON, N2T 0A4, Canada

[4] Department of Earth and Environmental Sciences, Syracuse University, Syracuse, NY, 13244, USA

[5] School for the Environment, University of Massachusetts Boston, Boston, MA, 02125, USA

[6] Hydrogeology Group, Institute of Geological Sciences, Freie Universität Berlin, Berlin, 12249, Germany

[7] Université de Corse Pascal Paoli, Département d'Hydrogéologie, Campus Grimaldi, Corte, 20250, France

[8] CNRS, UMR 6134 SPE, BP 52, Corte, 20250, France

Corresponding author: Lamine Boumaiza (lamine.boumaiza@uqac.ca)

ABSTRACT

The present study first describes the variations in concentrations of 12 chemical elements in groundwater relative to salinity levels in Southern Quebec (Canada) groundwater systems, and then uses this data to develop an empirical predictive model for evaluating groundwater chemical composition relative to salinity levels. Data is drawn from a large groundwater chemistry database containing 2,608 samples. Eight salinity classes were established from lowest to highest chloride (Cl) concentrations. Graphical analyses were applied to describe variations in major, minor, and trace element concentrations relative to salinity levels. Results show that the major elements were found to be dominant in the lower salinity classes, whereas Cl becomes dominant at the highest salinity classes. For each of the major elements, a transitional state was identified between domination of the major elements and domination of Cl. This transition occurred at a different level of salinity for each of the major elements. Except for Si, the minor elements Ba, B, and Sr, generally increase relative to the increase of Cl. The highest Mn concentrations were found to be associated with only the highest levels of Cl, whereas F was observed to be more abundant than Mn. Based on this analysis of the data, a correlation table was established between salinity level and concentrations of the chemical constituents. We thus propose a predictive empirical model, identifying a profile of the chemical composition of groundwater relative to salinity levels, to help homeowners and groundwater managers evaluate groundwater quality before resorting to laborious and costly laboratory analyses.

Keywords
Hydrogeochemistry, groundwater, salinity, major and minor elements, trace elements, Canada

1 INTRODUCTION

The uncontrolled exploitation of groundwater in combination with other anthropogenic activities has led to a severe deterioration of groundwater quality throughout the world (Seddique et al. 2019; Zendehbad et al. 2019; Boumaiza et al. 2020a). Geogenic processes also exert a significant impact on groundwater quality (Swartz et al. 2004; Bondu et al. 2018). Programs have been implemented throughout the world, at local, regional, and national scales, to assess and monitor groundwater quality and to evaluate the potential for anthropogenic and/or natural groundwater contamination (Leahy and Thompson 1994; Koreimann et al. 1996; Foster et al. 2006; Evans et al. 2012; Barbieri et al. 2019; Ricolfi et al. 2020). In Canada, several regional studies have recently been conducted with the aim of assessing the quality of groundwater in different provinces (e.g., Cui and Wei 2000; NBDE 2008; Kennedy and Drage 2009; Hamilton et al. 2015). In the Province of Quebec in Canada, where more than 2 million people rely on groundwater for their drinking water supply (Larocque et al. 2018), the assessment of regional groundwater quality is supported by the Groundwater Knowledge Acquisition Program (*Programme d'acquisition de connaissances sur les eaux souterraines*, PACES). This program was implemented in 2009 by the Quebec Ministry of the Environment (*Ministère de l'Environnement et de la Lutte contre les Changements Climatiques*, MELCC) to provide an integrated portrait of groundwater resources in Southern Quebec in terms of both quantity and quality, and to better protect and sustainably manage groundwater resources in Quebec (Rouleau et al. 2012; Larocque et al. 2018; MELCC 2021). The multi-faceted PACES program has developed alternative methods for assessing the vulnerability of aquifers, simulating groundwater flow, numerically estimating groundwater travel times, quantifying groundwater recharge, characterizing the internal architecture of aquifers, evaluating

85 specific aquifer properties, and understanding the chemical evolution of groundwater within
86 aquifers (Chesnaux et al. 2011; Boumaiza et al. 2015, 2017; Montcoudiol et al. 2015; Boumaiza
87 et al. 2019, 2020c, b, 2021a, c, b, 2022; Walter et al. 2017; Ferroud et al. 2018, 2019; Nadeau et
88 al. 2018; Chesnaux and Stumpp 2018; Labrecque et al. 2020).

89 The PACES program has provided insight into the wide variability of groundwater quality
90 in Southern Quebec, in both shallow unconfined aquifers and deeper confined aquifers. For
91 example, concentrations of chloride (Cl) in groundwater have ranged from values well below the
92 detection limit (<0.1 mg/L) to a very high value of 15,000 mg/L (MELCC 2021). Saline water that
93 is typically found in deeper aquifers (>1,000 m) is also found at shallow depths (<100 m) —both
94 in fractured rock and in unconsolidated aquifers— as the result of a long vertical upward flow
95 through discontinuities and faults (Rouleau et al. 2013; Wen et al. 2015). High Cl intake can cause
96 high levels of Cl in the bloodstream, a condition called hyperchloremia. Furthermore, at relatively
97 low concentrations, Cl can affect the taste of drinking water. In fact, when freshwater is mixed
98 with saltwater in as low a proportion as 1% (corresponding to ≈250 mg/L of Cl), it becomes unfit
99 for drinking (WHO 2017). Around the world, high salinity levels in groundwater have commonly
100 been associated with high levels of numerous inorganic chemical constituents (Deng et al. 2009;
101 Rango et al. 2013; Vikas et al. 2013; Avrahamov et al. 2014; Santucci et al. 2016; Elumalai et al.
102 2019) such as fluoride and boron; both of these can pose a health risk to humans at high
103 concentrations. Fluoride is a known xenobiotic; its impact on human health occurs through
104 fluorosis (Zango et al. 2019). Fluoride is suspected to be associated with other adverse health
105 effects, including ligament calcification, liver and kidney dysfunction, developmental disorder in
106 children, and neurological weakness (Ding et al. 2011; Yadav et al. 2019; Yang et al. 2020).

Exposure to large amounts of boron (approximately 30 g of boric acid) over short periods of time can affect the stomach, intestines, liver, kidney and brain and can eventually lead to death (ATSDR 2010).

In Quebec, a number of PACES-supported hydrogeochemical studies have reported the presence of high concentrations of various chemical constituents in groundwater (Beaudry, 2013; Blanchette et al., 2010b; Bondu et al., 2018, 2020; Chaillou et al., 2018; Meyzonnat et al., 2016; Minet et al., 2017; Montcoudiol et al., 2015; Walter et al., 2019). To fill in some of the remaining knowledge gaps, further studies are needed to draw a comprehensive portrait of the variations in concentrations of the different mineral constituents in groundwater, in particular relative to salinity levels. Knowledge of salinity levels is helpful for characterizing the flow, chemical evolution and mixing/migration patterns of groundwater within aquifer systems; it may also shed light on the vulnerability of groundwater to anthropogenic contamination (Grassi and Netti 2000; Williams et al. 2000; Lazur et al. 2020; Mora et al. 2020). Accordingly, the first objective of the present study is to describe the variability of chemical composition of groundwater in Southern Quebec in regards to its salinity levels. In this study, "chemical composition" of groundwater designates the concentration of inorganic elements in groundwater, whereas the term "salinity" refers to the Cl concentration (the terms "salinity" and "Cl concentration" are used interchangeably). Work on the first objective was based on the PACES groundwater chemistry database (MELCC 2021) which is comprised of data drawn from 2,608 groundwater samples collected in sixteen regions of Southern Quebec. The PACES database includes chemical analyses of 40 inorganic constituents. However, the present study focuses on Cl concentrations with 12 other inorganic constituents

128 (HCO_3^-, SO_4^{2-}, Ca^{2+}, Mg^{2+}, Na^+, K^+, B, Sr, Mn, Ba, Si, F) for which most measurements (>50%)
129 were reported above the detection limits of each inorganic element.

130 In Quebec, it is the legal responsibility of homeowners whose residence is not connected
131 to a municipal water supply (i.e., those who have their own well) to ensure the quality of their
132 groundwater; however, homeowners are not always able to assess groundwater quality and
133 undertake long-term monitoring owing to limited knowledge or financial means (Bondu et al.
134 2020). The second objective of the present study is therefore to develop an empirical groundwater
135 predictive model, to help gain preliminary insight into the quality of groundwater; such
136 information could be used to support a decision to avoid or pursue expensive chemical analyses.
137 The first objective, describing the variations in chemical concentrations and salinity levels in
138 groundwater in Southern Quebec, is used to achieve the second objective, which consists of
139 developing an empirical predictive groundwater quality model that establishes a relationship
140 between the chemical composition of groundwater and its salinity level. More specifically, by
141 linking Cl to electrical conductivity (EC), the model determines the Cl concentration of
142 groundwater based on the value of its EC, which can easily be measured in-situ. The relationship
143 between Cl and EC is established according to an empirical equation that was developed for this
144 study using the PACES groundwater chemistry data. Determining the salinity level then makes it
145 possible to predict the relative concentrations of the 12 studied chemical constituents influencing
146 the quality of groundwater. Assuming that PACES groundwater samples were collected under
147 equilibrium conditions, the resulting predictive model thus provides an empirical quantification,
148 in effect a “profile”, of the chemical composition of groundwater. Studies of groundwater systems
149 may include hydrochemistry numerical models, which require thermodynamic parameterization

150 including aquifer mineralogy. Such studies are extremely complex to conduct over large territories
151 such as Southern Quebec (100,000 km^2). An empirical predictive model such as the one proposed
152 in the present study may help draw a profile of groundwater quality and provide a useful step in
153 integrating and summarizing groundwater data collected over large geographic areas. The
154 predictive model is also a helpful tool to qualitatively monitor groundwater quality, to provide a
155 portrait of the chemical evolution of groundwater, and to manage groundwater in regard to its
156 salinity level.

157 **2 STUDY AREA**

158 2.1 **Location, climate and bedrock basement**

159 The study area encompasses sixteen administrative regions of Southern Quebec, Canada, covering
160 100,000 km^2 (indexed as 1 to 16 in Figure 1a). Southern Quebec, which has a humid northern
161 climate, experiences rainy events over the summer-fall seasons (from May-October), and heavy
162 snow accumulation during the winter-early spring seasons (from November to March), with
163 complete snowmelt occurring in April/May. The mean annual rainfall captured over Southern
164 Quebec is approximately 900 mm, with a mean annual snow accumulation equivalent to 290 mm
165 of water. The average monthly temperatures range from −16 °C in January to +18 °C in July
166 (Government of Canada 2021). The bedrock geology of the study area belongs to four geological
167 provinces (Figure 1b): (i) the Archean Abitibi greenstone belonging to the Southern part of the
168 Archean Superior Province (~4.3 to 2.5 billion years); (ii) the Grenville Province (~2.7 billion to
169 600 million years), which occupies a large portion of Southern Quebec; (iii) the St. Lawrence
170 Platform (~570 to 430 million years) extending in a northeastern orientation on both sides of the
171 St. Lawrence River; and (iv) the Appalachian Province (~480 million years) in the southeastern

172 part of the study area. Following the Wisconsin glacial retreat, when the glaciers deposited large
173 accumulations of Quaternary deposits (Figure 1c), southern Quebec was invaded by post-glacial
174 seas and proglacial lakes. These deposits are mainly composed of boulders, gravel, sand and clay-
175 silt, with thicknesses ranging from several meters to tens of meters (Bolduc and Ross 2001;
176 CERM-PACES 2013). The supply of drinking water in urbanized areas is usually drawn from
177 unconsolidated aquifers composed of granular sediments, rather than bedrock aquifers
178 (Dessureault 1975; Chaillou et al. 2018; Rey et al. 2018). However in rural areas, where single-
179 family dwellings largely rely on private domestic wells, bedrock aquifers are the major source of
180 drinking water (Montcoudiol et al. 2015; Meyzonnat et al. 2016; Walter et al. 2018).

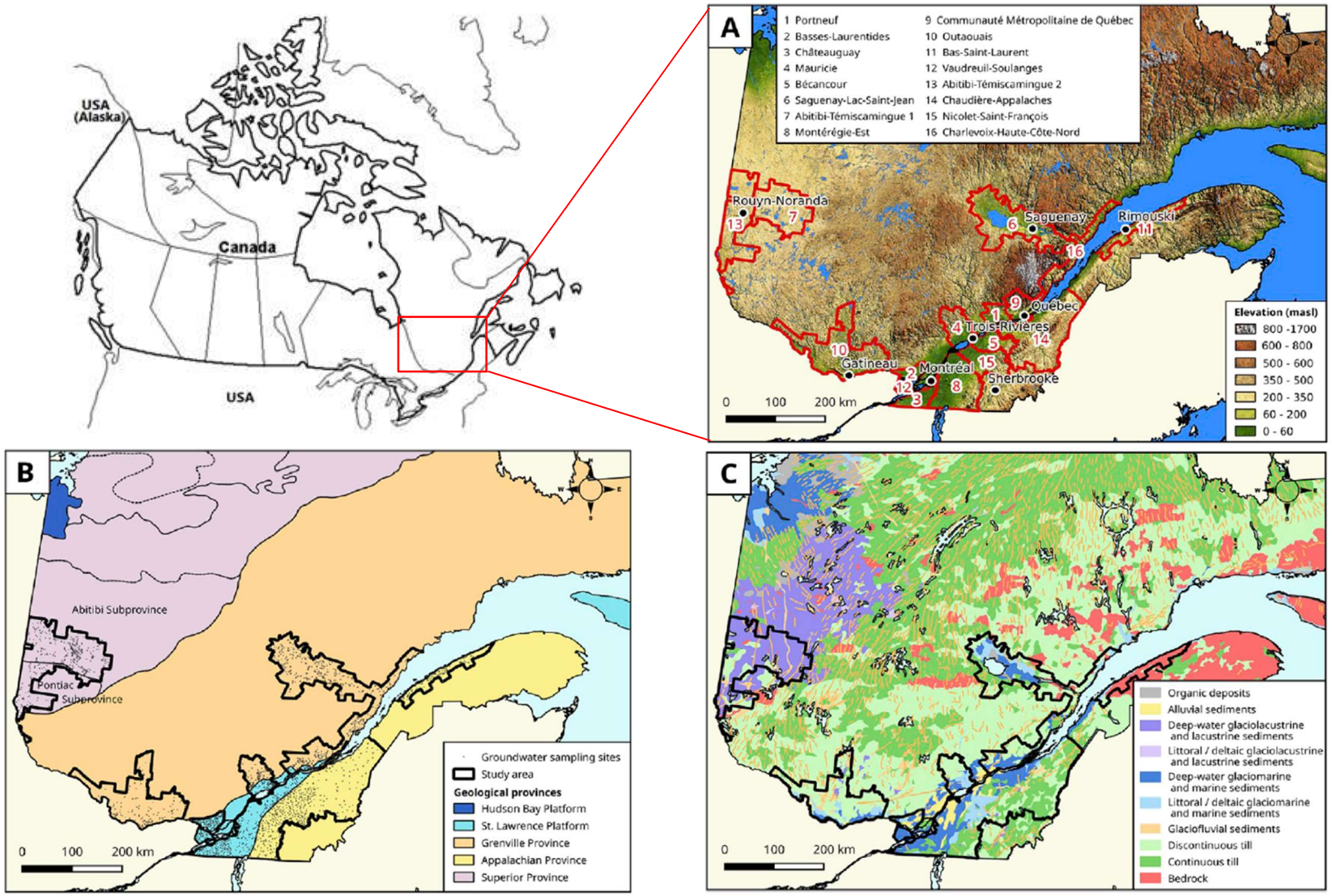

Fig. 1. (a) Location of the investigated study area in Quebec, Canada. The numbers 1-16 indicate the sub-regions of the study area, (b) Geological provinces, and (c) Surficial deposits (Bondu et al. 2020).

2.2 Hydrogeological and hydrogeochemical background

The coarse-grained sediment aquifers of the study area are commonly covered by glaciomarine and glaciolacustrine silt-clay deposits, forming confined aquifer systems (Dessureault, 1975; Lamothe and St-Jacques, 2014; Thibaudeau and Veillette, 2005). Granular sediments are also encountered in unconfined situations, as is the case with the major valleys of the Saguenay-Lac-Saint-Jean Highlands, which were not covered by fine sediments by the invading Laflamme Sea (Walter et al., 2018, 2017). Under the unconsolidated aquifers, the basement rocks are characterized by heterogeneous low permeabilities ranging from 10^{-9} to 10^{-4} m/s, wherein the groundwater flow is dominant in the fracture networks and bedding planes of the upper part (50–60 m) of the bedrock aquifers (McCormack and Therrien 2013; Rouleau et al. 2013; Benoit et al. 2014; Richard et al. 2016; Ladevèze et al. 2019). The bedrock aquifer systems are partly covered by silt and clay sediments, as in the case of glaciomarine clays in the St. Lawrence Lowlands, creating confining conditions for the bedrock aquifer systems (Lamothe 1989; Meyzonnat et al. 2016). In the Appalachian Highlands, however, surficial granular sediments are thin; therefore, unconfined conditions prevail for most of the fractured bedrock aquifer systems (Lefebvre et al. 2015). Recharge of the bedrock aquifer systems and the of the deeper unconsolidated aquifer systems occurs mostly in the unconfined areas typically found in highlands (Meinken and Stober 1997; Cloutier et al. 2006; Chesnaux 2013; Montcoudiol et al. 2015; Walter et al. 2017; Beaudry et al. 2018; Walter 2018).

In the highland recharge areas, groundwater is characterized by low mineralization, a slightly acidic to near neutral pH and oxidizing redox potential, in which the dominant water type is Ca-HCO_3. This is consistent with water that has recently infiltrated into the subsurface, whose

features are governed by weathering of silicate (Ca-feldspar, particularly) (Beaudry et al., 2018; Chaillou et al., 2018; Ghesquière et al., 2015). This groundwater type evolves to Na-HCO_3 during subsurface migration and interacts with the post-glacial marine clay (Montcoudiol et al. 2015; Walter et al. 2019); it can be found in the semi-confined to confined aquifers under reducing conditions, as identified, for example, in the confined aquifers of south-western Quebec (Meyzonnat et al. 2016), and in the confined bedrock aquifers of the Saguenay-Lac-Saint-Jean region (Walter et al. 2017). The chemistry of groundwater tends to evolve further toward modern seawater-like compositions, i.e., Na-Cl-rich (Walter et al. 2017). This Na-Cl water type — characterized by high total dissolved solids, alkaline pH and mildly reducing to reducing redox potential— mainly occurs in confined unconsolidated/bedrock aquifers, and is widely prevalent in the study area (Cloutier et al. 2008, 2010; Ghesquière et al. 2015; Lefebvre et al. 2015; Montcoudiol et al. 2015).

3 MATERIALS AND METHODS

3.1 Data overview

The PACES database contains data drawn from a total of 2,608 groundwater samples collected from private, municipal and observation wells during the summer periods as part of the 2009-2015 PACES Program; 893 samples were collected from unconsolidated aquifers and 1,678 groundwater samples were obtained from bedrock aquifers (37 of the 2,608 samples originated from an unknown aquifer type). All groundwater samples collected in the PACES Program were analyzed by an accredited commercial laboratory (*Bureau Veritas Laboratories*) in compliance with the standard procedures of Quebec's Ministry of the Environment (CEAEQ 2021). Laboratory analyses targeted major elements (Cl, HCO_3, SO_4, Ca, Mg, Na, K) and some minor

228 and trace elements (B, Sr, Mn, Ba, Si, F). Alkalinity (as $CaCO_3$) and HCO_3 were determined by
229 volumetric titration to pH 4.5 using a Mantech (Guelph, ON) PC-Titrate auto-analyzer. The anions
230 SO_4 and Cl were measured using a Dionex (Sunnyvale, CA) ICS-1600 ion chromatograph. Major
231 cations (Ca, Mg, Na, K), and minor/trace elements (Si, B, Ba, Mn, Sr) were analyzed by
232 inductively coupled plasma mass spectrometry (ICP-MS) using an Agilent (Santa Clara, CA)
233 7700X ICP-MS. Fluoride (F) was measured using a fluoride ion-selective electrode (a complete
234 description of each analytical method employed is available in CEAEQ (2021)). In the present
235 study, values below the detection limit for each of the 13 selected chemical constituents were not
236 included in the statistical analyses, to avoid including unreliable values in the statistical analysis.
237 Quality-Assurance/Quality-Control programs were implemented that considered both field and
238 laboratory procedures —in compliance with the standard procedures of Quebec's Ministry of the
239 Environment (CEAEQ 2021)— with the calculation of ionic balance, for which a value of ±10%
240 is considered acceptable (Hounslow 1995). The procedures included field and transport blanks,
241 which were performed to evaluate a potential contamination from the field and/or during
242 transportation of groundwater samples. Furthermore, field procedures included the collection of
243 duplicate groundwater samples (DGSs) corresponding to 10% of the total collected groundwater
244 samples. The DGSs were collected at the same time as the initial groundwater samples (IGSs),
245 from same sampling origin, and sent to the laboratory under different identifications that those of
246 the IGSs. Further, the collected DGSs were analyzed for selected inorganic elements, while their
247 results were compared to those of the IGSs. Similar procedures were performed by the laboratory,
248 which performed twice analyses for 10% of the total received IGSs, in order to evaluate the
249 replicability of the analysis procedure. The standard deviation (STD) between DGS and IGS

250 results was calculated. The STD was generally considered acceptable at ≤10%. When a STD >10%
251 was noted, the results were considered only as estimates of the actual concentration. However,
252 when the chemical results show relatively low values, i.e., ≤5 times the detection limit, the STD
253 cannot be significantly evaluated. Quality-Assurance/Quality-Control results indicated STD
254 values within 10%, confirming the replicability of the analyses, while the analytical results were
255 validated by testing the ionic balance, for which values of ±10% were obtained overall.

256 3.2 **Determination of salinity classes**

257 To discuss the variations in chemical composition of groundwater in terms of its Cl levels, classes
258 of salinity were determined. The Cl concentrations of the groundwater samples range from 0.003
259 to 423 meq/L (0.1 to 15,000 mg/L). The inflection points on the cumulative density curve of Cl
260 concentrations (i.e., plotting the probability of a sample concentration relative to a sample set) are
261 considered to be the thresholds limiting the different salinity classes (Oberhelman and Peterson
262 2020). Because the present study did not aim to determine salinity classes by distinguishing
263 between aquifer types or even geological provinces, all 2,608 groundwater samples were
264 considered in this analysis, regardless of their underlying lithology or aquifer type.

265 3.3 **Statistical analysis**

266 Within each salinity class, the concentrations of each chemical constituent are presented in a box-
267 and-whisker diagram (boxplot), which includes the statistical upper quartile (Q3; 50–75% above
268 the median) and the lower quartile (Q1; the lowest 25% of numbers), the median, the maximum
269 (elevated), and minimum (lower) concentrations of each chemical constituent. For each of the 12
270 investigated chemical constituents, the boxplot results —relative to salinity class— are described.
271 Furthermore, the median value of each boxplot is used for determining the trend of the variation

in the chemical concentration of groundwater; the Mann-Kendall test (Mann 1945; Kendall 1975), integrated into the XLSTAT software (Addinsoft 2021), was used for this purpose. The null hypothesis (H_0) of the Mann–Kendall test indicates no trend, whereas the alternate hypothesis (H_a) indicates either an upward or a downward trend. A positive Kendall Ꞇ corresponds to an upward trend, whereas a negative Kendall Ꞇ indicates a downward trend (Pohlert 2020).

3.4 **Development and validation of the predictive model**

We propose a groundwater predictive model able to determine the chemical profile of groundwater. This proposed predictive model may be a helpful tool for homeowners and/or groundwater managers to gain insight into the quality of a groundwater via a simple and direct measurement of its EC. This predictive model can also be used to screen groundwater samples in order to determine which among them may require more comprehensive chemical analyses; such early determination may help avoid unnecessary testing, which tends to be costly and time-consuming. The model achieves this discrimination based on the identification of the salinity class of a groundwater sample. The salinity class for a given groundwater sample can be determined from the direct in-situ measurement of the groundwater EC, using an equation proposed in the present study that establishes a link between the Cl concentration and the EC (EC data is included in the PACES chemical database). The predictive model contains a series of chemical constituents; to each of these corresponds a representative value according to each salinity class. The representative value of each chemical constituent was established through a boxplot statistical analysis. The median values of the boxplot were adopted for the proposed model, rather than the outlier values, as the median values are more representative of a dataset.

The validation of the proposed predictive model was carried out by comparing the established median value of each of the 12 chemical constituents in the predictive model against equivalent control values drawn from another data source (i.e., other groundwater samples collected during the PACES Program that were not a part of the 2009-2015 PACES data used in the present study but taken from the 2018-2022 PACES Projects). Validation was a three-step process. Firstly, the Cl concentrations in groundwater samples from the control data were determined by using an equation linking the Cl concentration to the EC, which was measured *in situ*. Secondly, the control groundwater samples were classified and grouped according to their salinity level determined from their calculated Cl concentration. Thirdly, the median value —of each of the 12 chemical constituents— of each determined salinity class (actual value) is compared to the chemical constituent value of the predictive model (predicted value). Here, the correlation between the actual and predicted values is used to judge the predictive model efficiency.

4 DESCRIPTION OF RESULTS

4.1 Salinity classes

Based on the inflection points in the cumulative density curve of Cl in groundwater, six salinity intervals were initially established (Figure 2a). However, because the Cl interval from 12.4 to 423 meq/L (i.e., 440 to 15,000 mg/L) was very large in terms of Cl concentration, it was refined by graphically detecting sub-inflection points (Figure 2b). The inflection points are represented as points connecting different slopes on the cumulative density curve. Thus, a total of eight salinity classes were considered for the present study (Table 1).

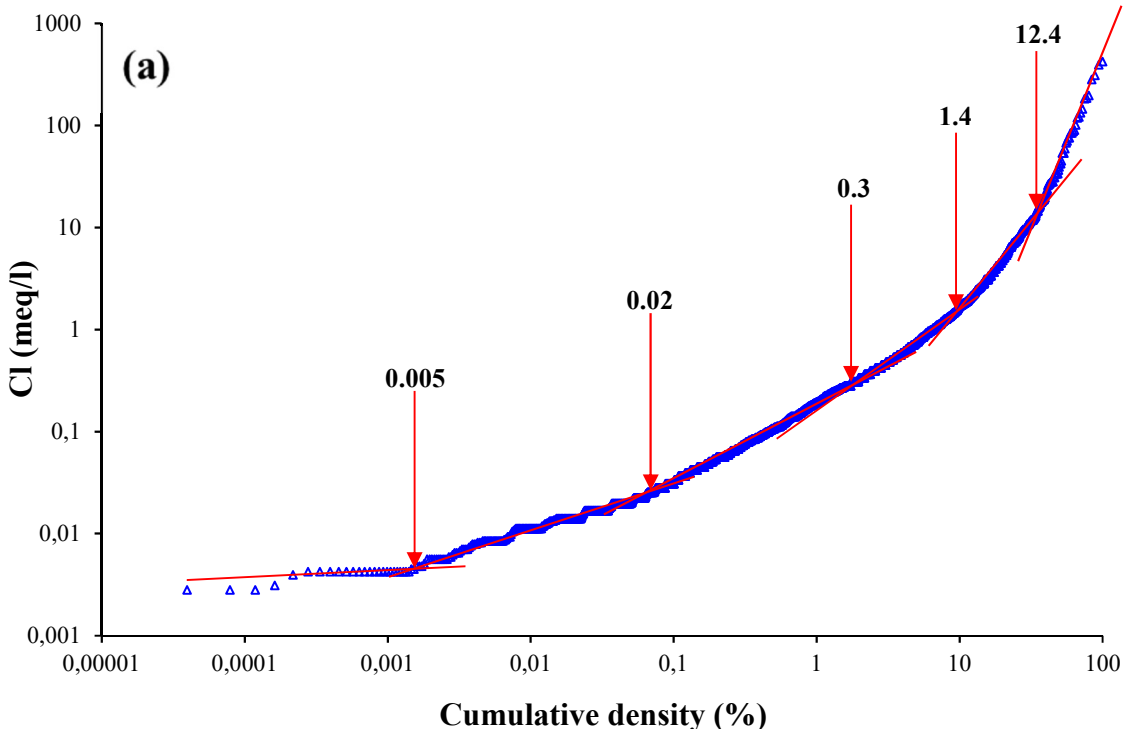
(a)
1000
100
10
1
0,1
0,01
0,001
Cl (meq/l)
0,00001
0,0001
0,001
0,01
0,1
1
10
100
Cumulative density (%)
0.005
0.02
0.3
1.4
12.4

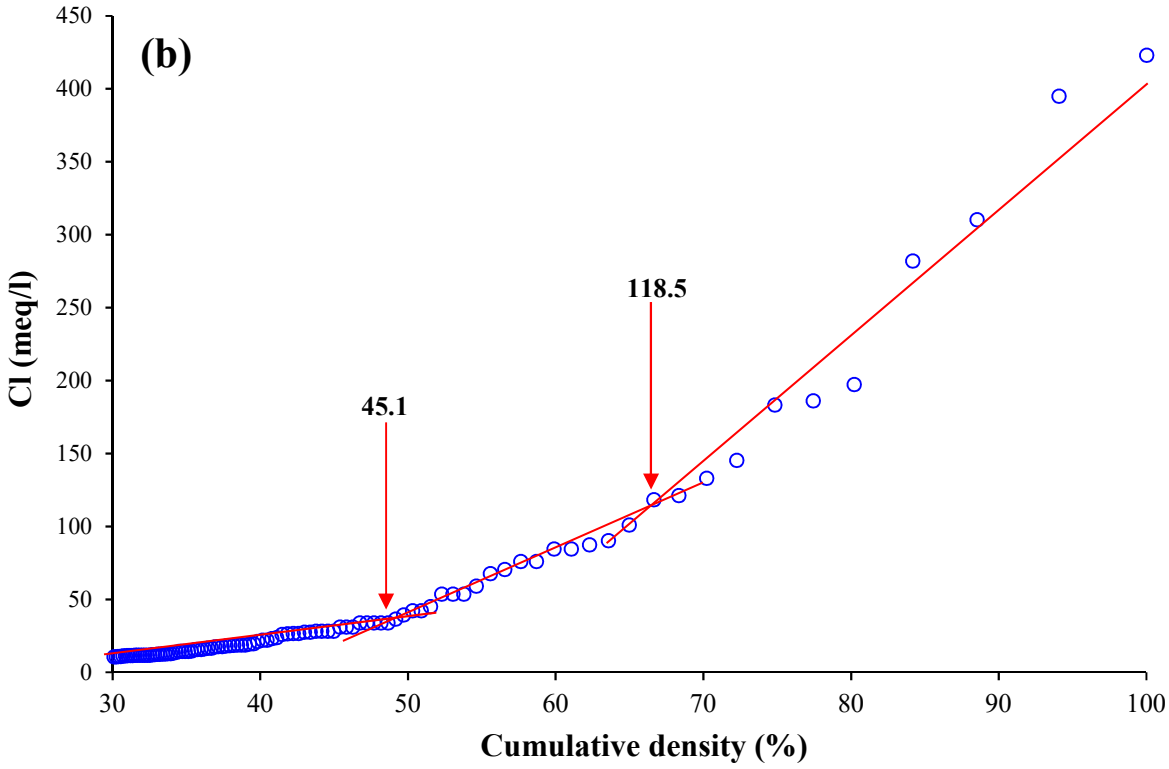
(b)
450
400
350
300
250
200
150
100
50
0
Cl (meq/l)
30
40
50
60
70
80
90
100
Cumulative density (%)
45.1
118.5

Fig. 2. Cumulative density curves for the Cl concentration in groundwater. In (a), the data are expressed by log scale because the interval of cumulative density values is too large from 0.00001 to 100; whereas in (b) the data are expressed by a linear scale as the cumulative density is small (from 30 to 100) compared to that illustrated in (a).

Table 1. Thresholds of salinity classes of the PACES dataset.

Salinity class	Interval (meq/L)	Interval (mg/L)	Samples (*n*)
1	<0.005	<0.16	25
2	0.005–0.02	0.16–0.8	260
3	0.02–0.3	0.8–10	978
4	0.3–1.4	10–50	775
5	1.4–12.4	50–440	429
6	12.4–45.1	440–1,600	57
7	45.1–118.5	1,600–4,200	14
8	>118.5	>4,200	11

4.2 **Distribution of the chemical constituents within salinity classes**

4.2.1 ***Distribution of major anions***

The boxplot statistical distribution of HCO_3 and SO_4 concentrations, from the dataset of 2,608 groundwater samples, is shown in Figures 3a and b, respectively. The median HCO_3 concentrations overall revealed an increasing trend that was confirmed by a positive Kendall Ꞇ with p-value <0.05 (see supplementary material). The median HCO_3 values show an increase starting from 0.9 meq/L (53 mg/L) at salinity class 1 (Cl <0.005 meq/L) to a value of 6.1 meq/L (374 mg/L) at salinity class 6 (Cl = 12.4−45.1 meq/L) (Figure 3a). However, for Cl >45.1 meq/L, the median HCO_3 concentrations show a decrease relative to the increase in Cl concentration (Figure 3a). In Figure 3a, the median HCO_3 concentrations in salinity classes 1−4 (Cl <1.4 meq/L; i.e., 50 mg/L) are greater than the corresponding Cl concentrations, suggesting a dominance of HCO_3 in salinity classes 1−4 (dominance of chemical element compared to another one means here that its concentration is greater than that of the compared element). Conversely, for Cl

concentrations >12.4 meq/L (>440 mg/L) in salinity classes 6−8, the median HCO_3 concentrations are lower than the corresponding Cl concentrations of classes 6−8. This observation suggests a dominance of Cl for the samples belonging to these classes 6−8. Salinity class 5 (Cl = 1.4−12.4 meq/L) represents a transition from HCO_3-dominant to Cl-dominant; it has a median HCO_3 concentration of 4.3 meq/L (262 mg/L), which is within the Cl variation interval of salinity class 5 (Cl = 1.4−12.4 meq/L), confirming a transitional state from HCO_3-dominant to Cl-dominant. The interquartile interval of HCO_3 (i.e., difference between the lower and upper quartiles) progressively increases through salinity classes 1−8 (except class 7), suggesting an increasing variation in HCO_3 concentration relative to the increase in Cl concentration.

Unlike HCO_3, the median SO_4 concentration (Figure 3b) consistently increases through the eight salinity classes; this is also confirmed by a positive Kendall Ƭ with p-value <0.05 (see supplementary material). The greatest SO_4 increase between salinity classes was observed between classes 7 (Cl = 45.1−118.5 meq/L) and 8 (Cl >118.5 meq/L), with a median SO_4 concentration increasing from 2.5 meq/L (120 mg/L) to 35 meq/L (1,700 mg/L). The SO_4 interquartile interval (Figure 3b) progressively increases from salinity class 1 to 8, suggesting that the variability of SO_4 concentrations is in correlation with the increase in Cl concentrations. In salinity class 8, the maximum/minimum SO_4 concentrations (i.e., the whisker outlier values) are close to the first and third quartiles (Figure 3b). This indicates that, despite having the largest interquartile interval, class 8 has a narrow variation of SO_4 relative to interquartile interval limits. The median SO_4 concentrations through salinity classes 1−2 are greater than the corresponding Cl concentrations of classes 1−2, suggesting SO_4 dominance over Cl in salinity classes 1−2 (Figure 3b). In contrast, for Cl concentrations >1.4 meq/L (>50 mg/L), corresponding to salinity classes 5−8, the median

356 SO_4 concentrations are lower than the corresponding median Cl concentrations. This suggests that
357 Cl is dominant over SO_4 in salinity classes 5−8. Salinity classes 3 and 4 correspond to median SO_4
358 concentrations of 0.2 and 0.4 meq/L, which are within the Cl variation interval of salinity classes
359 3 (Cl = 0.02−0.3 meq/L) and 4 (Cl = 0.3−1.4 meq/L). For this reason, salinity classes 3 and 4 may
360 be considered as transitional between groundwater dominated by SO_4 to groundwater dominated
361 by Cl.

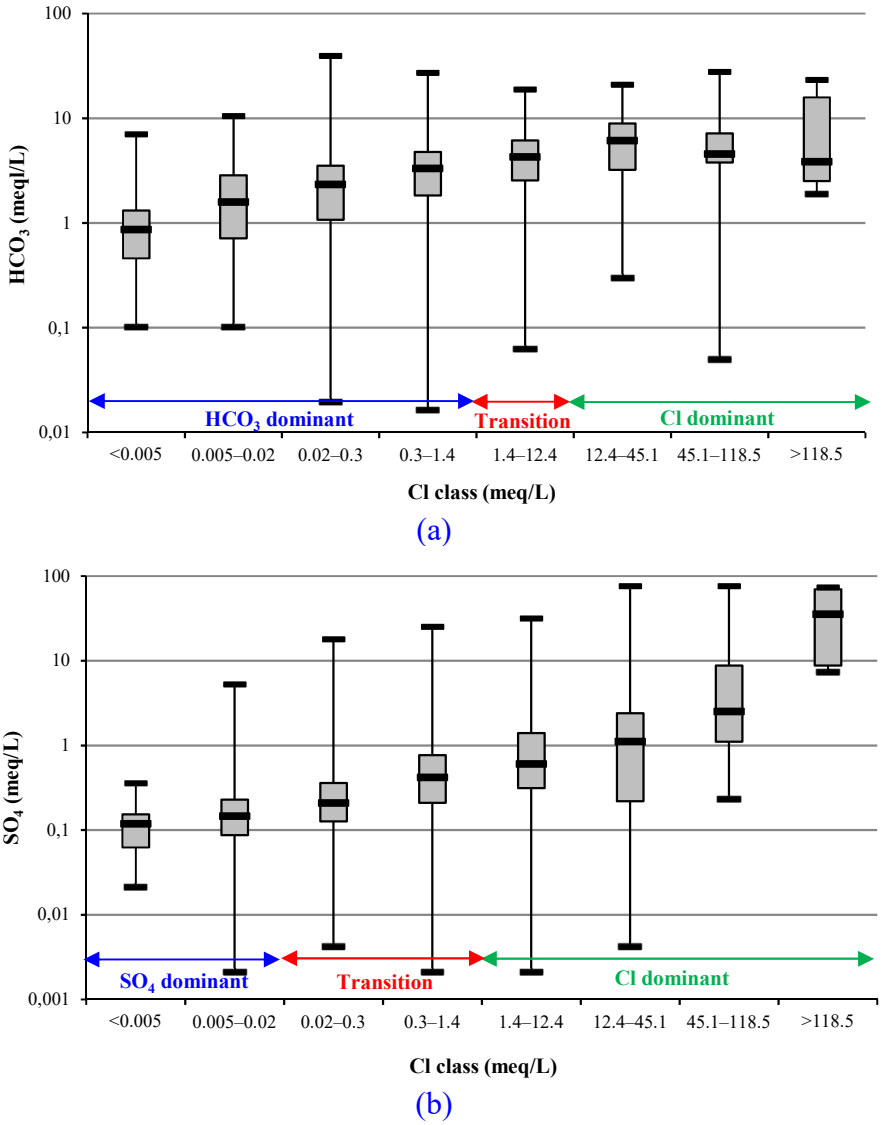

362 Fig. 3. Boxplot distribution of major anions over the Cl classes: (a) HCO_3 and (b) SO_4.

363 *4.2.2* ***Distribution of major cations***

364 Figures 4a, b, c, and d show that the concentrations of each of the major cations increase as Cl
365 concentration increases; an observation confirmed with a positive Kendall Ƭ (see supplementary
366 material). In Figure 4a, groundwater samples through salinity classes 1−4 are dominated by Ca, as
367 Ca median values (0.8, 1, 1.5 and 2 meq/L) are greater than the Cl concentration corresponding to
368 salinity classes 1−4. Inversely, classes 6−8 are found to be dominated by Cl. Salinity class 5
369 corresponds to a median Ca concentration of 2.3 meq/L, which is within the Cl variation interval
370 of salinity class 5 (Cl = 1.4−12.4 mg/L). Hence, salinity class 5 corresponds to a transition between
371 groundwater dominated by Ca to groundwater dominated by Cl. The median Mg values (Figures
372 4b) are observed to overlap the Cl concentration in salinity classes 1−3; therefore, there is a
373 tendency for dominance of magnesian water types in these salinity classes 1−3. Salinity class 4
374 corresponds to a median Mg concentration of 0.7 meq/L, which is within the Cl variation interval
375 of salinity class 4 (Cl = 0.3−1.4 meq/L). This suggests that salinity class 4 also represents a
376 transition. Indeed, Cl concentrations in classes 5−8 are greater than the corresponding median Mg
377 concentrations, suggesting, in this case, the dominance of Cl over Mg.

378 The median K values (Figures 4d) show that groundwater samples in salinity classes 1−2
379 are dominated by potassic water type, as K median values are greater than Cl concentration,
380 corresponding to salinity classes 1−2. Inversely, classes 4−8 have Cl concentrations greater than
381 K concentrations, suggesting Cl water type dominance across these classes. Salinity class 3
382 corresponds to a median K concentration of 0.04 meq/L, which is within the Cl variation interval
383 of salinity class 3 (Cl = 0.02−0.3 mg/L); therefore, salinity class 3 corresponds to a transition
384 between groundwater dominated by K to groundwater dominated by Cl. In Figure 4c, the median

385 Na concentrations through classes 1 (Na = 0.07 meq/L) and 2 (Na = 0.16 meq/L) are found to be
386 greater than the corresponding Cl concentrations of classes 1 (Cl <0.005 meq/L) and 2 (Cl =
387 0.005−0.02 meq/L), respectively. Hence, Na is dominant over classes 1−2. For Cl concentrations
388 >118.5 meq/L (class 8), the median Na concentration (173.3 meq/L) is greater than 118.5 meq/L.
389 However, this does not indicate that Na is dominant with respect to Cl, as class 8 includes Cl
390 concentrations even greater that 173.3 meq/L, and appropriately suggest that Cl is dominant over
391 Na in this salinity class 8. Classes 3−7 correspond to median Na concentrations that are within the
392 Cl variation interval of the corresponding salinity classes. Hence, classes 3−7 constitute a transition
393 from groundwater dominated by Na to groundwater dominated by Cl.
394 In this study, median Ca concentrations (Figure 4a) are observed to be higher than median
395 Na concentrations (Figure 4c) for Cl concentrations <1.4 meq/L (<50 mg/L), i.e., over classes 1−4.
396 For Cl >1.4 meq/L (i.e., over classes 5−8), Na concentrations become inversely dominant over Ca.
397 The median Ca concentration corresponding to salinity class 6 (1.6 meq/L) was found to be slightly
398 lower than that of the preceding class 5 (2.3 meq/L). The Na concentrations over classes 5−6
399 increase substantially from 3.8 to 21.8 meq/L. As Na concentrations are dominant over Ca
400 concentrations in the highest salinity classes (classes 5−8), groundwater samples having the
401 highest salinity are generally of the Na-Cl water type.
402

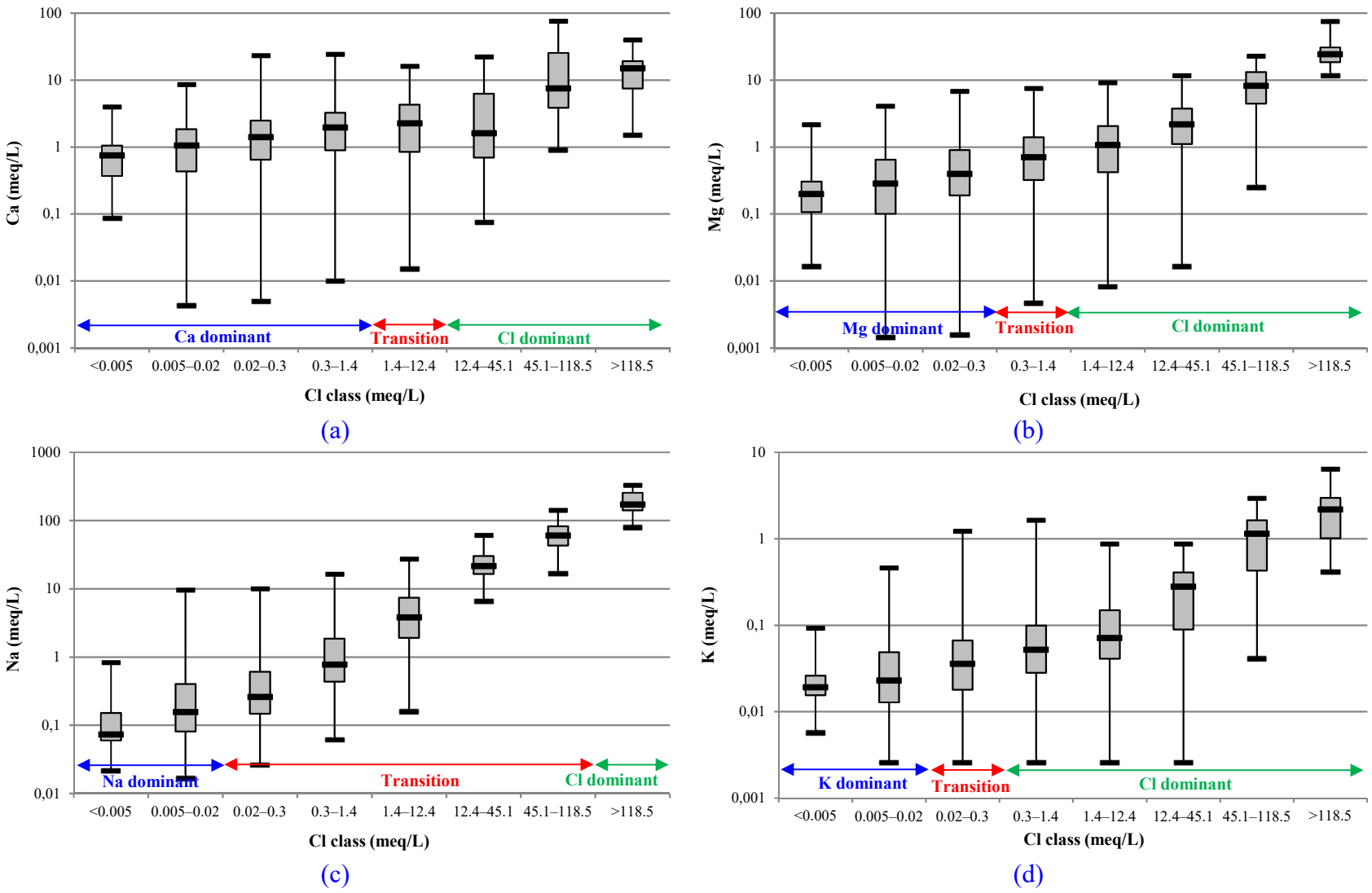

Fig. 4. Boxplot distribution of major cations over the Cl classes: (a) Ca, (b) Mg, (c) Na and (d) K.

403

4.2.3 ***Distribution of minor elements B, Ba, Sr and Si***

The boxplot statistical distributions of the four minor elements B, Ba, Sr, and Si, relative to the Cl concentration (in mg/L), are shown in Figures 5a, b, c, and d, respectively. Boron, Ba, and Sr concentrations generally increase as the Cl concentration increases. This observation is confirmed through the positive Kendall Ꞇ presented in the supplementary material. Strontium shows the most pronounced increase in concentration, with median values ranging from 0.04 (salinity class 1: Cl <0.16 mg/L) to 18 mg/L (class 8: Cl >4,200 mg/L). It appears that relative to the increase in Cl, there is a no regular enrichment of Ba and B compared to Sr. The median Ba concentrations in salinity classes 1−5 (median Ba = 0.007, 0.016, 0.04, 0.07, and 0.1 mg/L) are comparable to median B concentrations in each corresponding class (median B = 0.007, 0.014, 0.03, 0.04, and 0.1 mg/L). In salinity classes 6−7 (Cl 440−4,200 mg/L), median B concentrations (median B = 0.35 and 0.66 mg/L) are higher than Ba (median Ba = 0.18 and 0.22 mg/L). For the highest Cl concentration class (class 8: Cl >4,200 mg/L), the median Ba concentration (2 mg/L) is found to be higher than the B concentration (1.3 mg/L). Also, the maximum Ba concentration (12 mg/L) is observed to be significantly higher than the maximum B concentration (3.5 mg/L). B is dominant over Ba in groundwater samples having a Cl concentration ranging from 440 to 4,200 mg/L, whereas Ba becomes dominant over B when the Cl concentration in groundwater is >4,200 mg/L. Through salinity classes 1−7, the median Si concentrations show a very slight variation ranging from 6 to 9 mg/L (Figure 5d), suggesting that Si has limited sensitivity to salinity variation. Indeed, the Mann-Kandel result related to Si (see supplementary material) indicates that the Si trend is not statistically significant with a p-value of 0.105 greater than the confidence level of 0.05.

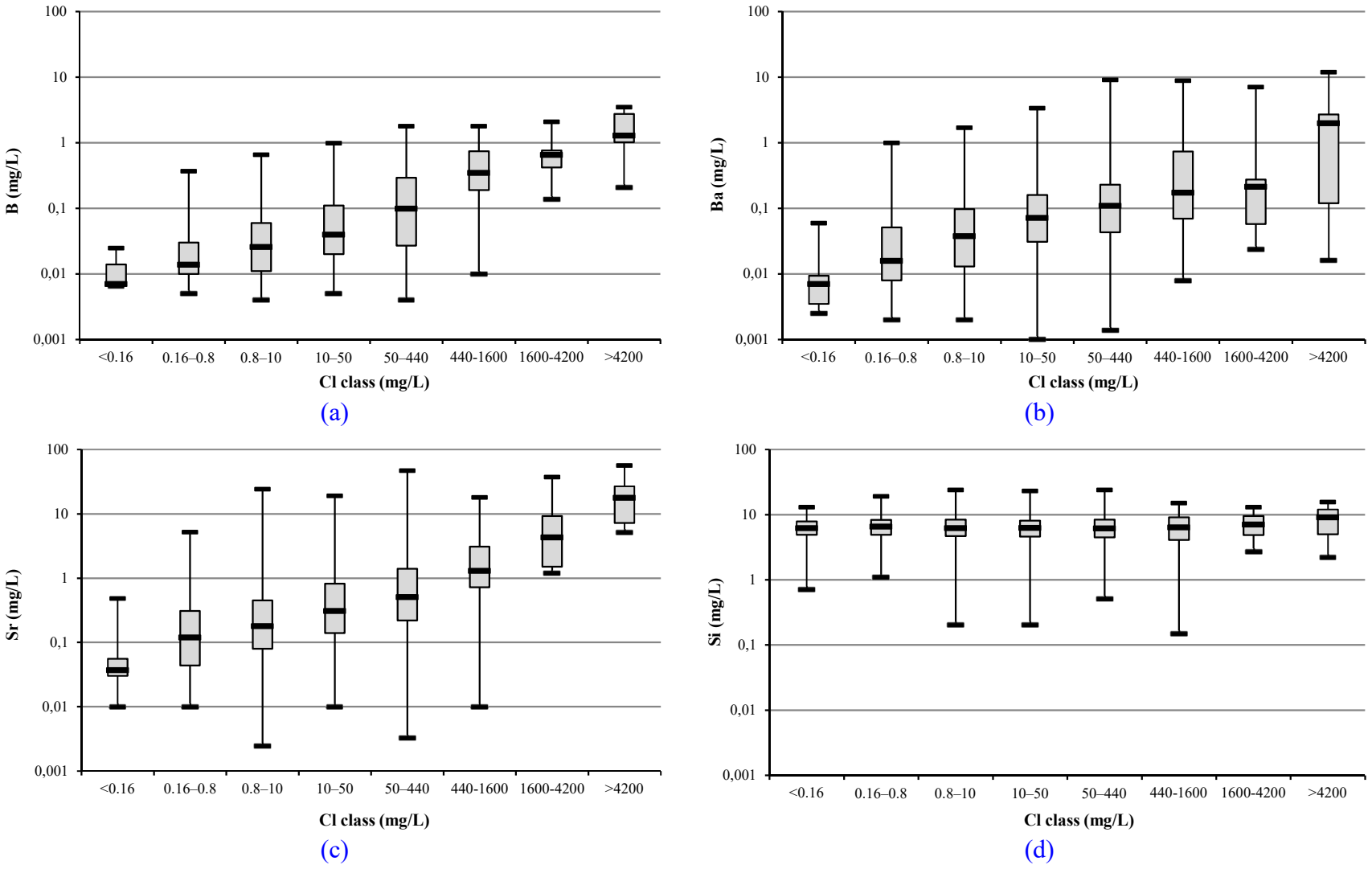

426 Fig. 5. Boxplot distribution of minor elements over the Cl classes: (a) B, (b) Ba, (c) Sr, (d) Si.

4.2.4 ***Distribution of trace elements Mn and F***

Two trace chemical elements are considered in the present study, Mn and F, because elevated concentrations of these elements in groundwater can exert a significant impact on the quality and drinkability of groundwater with regards to human health. In several studies conducted in Southern Quebec, concentrations of Mn and F in groundwater have exceeded Canadian standards for drinking water (acceptable limits are Mn = 0.12 mg/L; F = 1.5 mg/L) (Montcoudiol et al. 2015; Saby et al. 2016; Walter et al. 2017; Bondu et al. 2020; Health Canada 2020). In this study, the median Mn concentrations are lower than 0.1 mg/L for groundwater Cl concentrations <4,200 mg/L (classes 1−7), and the lowest/highest Mn median concentrations are observed for the lowest/highest Cl concentrations (Figure 6a). The median Mn concentration is observed to be generally constant (0.02 mg/L) over salinity classes 1−6, while in classes 7−8, median Mn concentrations increase to reach a value of 0.4 mg/L. The increase in Mn concentration is mostly limited to high Cl concentrations, which may explain the modest trend of Mn concentrations with p-value of 0.048 (see supplementary material). For Cl concentrations <50 mg/L (classes 1−4), the Mn concentration of groundwater samples in the 3rd quartile (Figure 6a), are above the maximum acceptable level of Mn in drinking water (0.12 mg/L), whereas the 1st quartile groundwater samples have Mn concentrations below the acceptable limit (Figure 6a). Median F concentrations range from 0.1–0.8 mg/L, and do not exceed 1 mg/L through all salinity classes (Figure 6b). Median F concentrations over salinity classes 1–4 (Cl = 0.16–50 mg/L) do not show significant variation, with a value of 0.2 mg/L. Subsequently, the median F concentrations increase as Cl concentrations increase, reaching a value of 0.8 mg/L in saline class 8 (Cl >4,200 mg/L), justifying the positive F-Kendall Ƭ with a p-value <0.05 (see supplementary material). In Figure 6b, the 3rd quartile groundwater samples show F concentrations

449 below the Canadian drinking water standard of 1.5 mg/L through all the salinity classes, except
450 salinity class 6 (Cl = 440–1,600 mg/L) for which the 1st quartile groundwater samples are below the
451 standard of 1.5 mg/L.
452

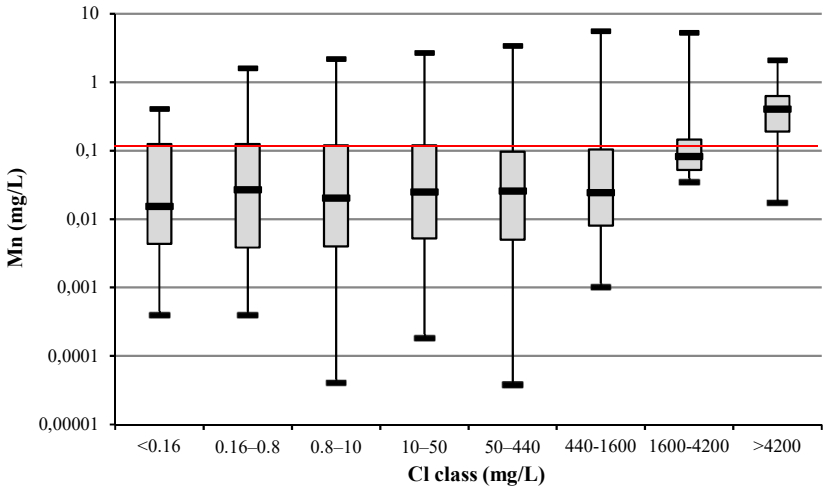

(a)

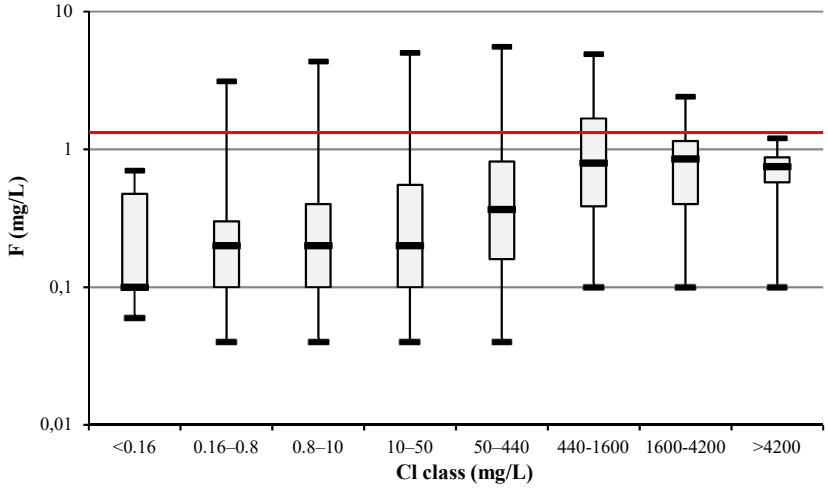

(b)

453 Fig. 6. Boxplot distribution of trace elements (a) Mn and (b) F in the Cl classes. The red line
454 indicates the maximum acceptable concentrations of these elements in Canadian drinking water.
455
456
457

5 Presentation and validation of the proposed empirical predictive model

To propose an empirical predictive model of the concentrations of the chemical constituents in groundwater relative to the concentrations of Cl, the median values (expressed in mg/L) of the 12 chemical constituents investigated in this study were considered. Table 2 summarizes the median concentrations of these chemical constituents relative to the Cl concentration expressed in mg/L (salinity classes). Table 2 constitutes the predictive model that makes it possible to determine the chemical profile of groundwater relative to the Cl level. This predictive model is proposed to help homeowners/groundwater managers gain valuable insight regarding groundwater quality prior to costly laboratory analyses. To apply the predictive model to a given groundwater sample, the methodology, first, consists of determining the EC of the groundwater sample; this is easily done *in situ* in the field. Secondly, based on the value of the groundwater EC, calculate the value of groundwater Cl concentration using an equation linking Cl to EC. Equations linking Cl to EC have been proposed in the literature (e.g., Howard and Haynes 1993; Meriano 2007). Following a similar approach, the best relationship according to the Southern Quebec groundwater database employed in this study is: $Cl = 0.0047 \times EC^{1.4273}$ (equation developed based on the fitted linear relationship of Cl in mg/L with EC in µS/cm). Once the Cl concentration of groundwater sample is calculated from the EC, thirdly, the use of Table 2 allows to determine the salinity class, corresponding to the determined Cl concentration, to which a groundwater sample belongs. Knowing the salinity class makes it possible to determine the chemical profile of a groundwater sample by predicting the relative concentrations of the chemical constituents. Figure 7 summarizes the successive steps of the proposed survey methodology approach. In certain situations, this model may provide preliminary information on groundwater that either makes it possible to avoid resorting to laboratory

chemical analyses, or on the contrary, indicates the need to proceed with further analyses. The predictive model proposed in the present study was developed using data drawn from the PACES groundwater chemistry and may, therefore, be appropriately applied to the regions of Southern Quebec. However, the methodology used to develop this predictive model may be applied to datasets drawn from other groundwater databases, to predict groundwater chemical profile in other regions. In the present study, the groundwater predictive model is limited to 12 inorganic chemical constituents (HCO_3, SO_4, Ca, Mg, Na, K, Ba, B, Sr, Si, Mn, and F), but can be extended in other studies to other chemical constituents.

Table 2. Predictive model to determine groundwater chemical profile based on salinity level: Correlation between the salinity levels of groundwater and the concentrations of 12 chemical constituents (developed using the 2009-2015 PACES Program data).

			Salinity class							
			1	**2**	**3**	**4**	**5**	**6**	**7**	**8**
			Cl concentration (mg/L)							
Group	**Element**	**Stand. ***	**<0.16**	**0.16–0.8**	**0.8–10**	**10–50**	**50–440**	**440–1,600**	**1600–4,200**	**>4,200**
Anions	HCO_3	200	53	95	134	202	261	374	278	235
	SO_4	200	6	7	10	20	29	50	120	1700
Cations	Ca	75	15	21	28	39	45	32	135	300
	Mg	30	2	3	5	9	13	27	100	294
	Na	200	2	4	6	18	88	500	1400	3981
	K	12	0.75	0.90	1.40	2.05	2.80	11	45	85
Minor and trace elements	B	5	0.007	0.014	0.025	0.04	0.1	0.35	0.66	1.3
	Ba	1	0.007	0.016	0.038	0.072	0.11	0.18	0.22	2
	Sr	7	0.04	0.12	0.18	0.31	0.51	1.3	4.3	17.8
	Si	-	6.2	6.6	6.2	6.3	6.2	6.4	7.05	9.15
	Mn	0.12	0.0155	0.025	0.019	0.024	0.026	0.025	0.083	0.41
	F	1.5	0.1	0.2	0.2	0.2	0.4	0.8	0.8	0.7

** Drinking water limit concentration in mg/L* (WHO 2017; Government of Canada 2021).

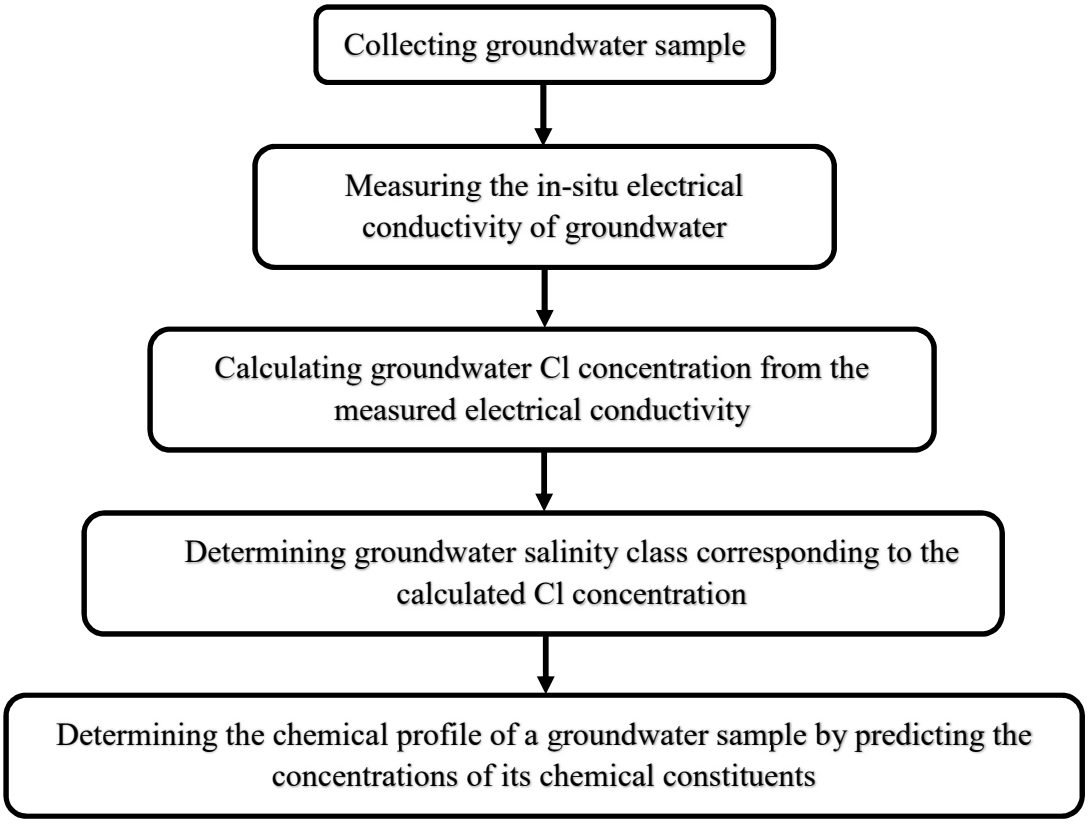

Fig. 7. Successive steps of the proposed survey methodology approach.

The validation of the predictive model (Table 2) was undertaken by applying the established salinity classes to an independent dataset. The objective of the validation was to verify whether the concentrations predicted by the model for a given groundwater samples match the actual concentrations that were measured. For this purpose, we used the results of an independent chemical analysis of 313 groundwater samples drawn from a different dataset than the dataset used to develop the predictive model. These independent groundwater samples were collected from the Mauricie-2 and Lanaudière regions belonging to Southern Quebec (Tremblay et al. 2021) and analyzed for different inorganic constituents including the 12 elements: Ca, Mg, Na, K, HCO_3, SO_4, B, Sr, Mn,

Ba, Si, and F. The validation approach started by categorizing the 313 groundwater samples according to their Cl concentration into one of the 8 predetermined salinity classes indicated in Table 1. The Cl concentrations of these independent groundwater samples ranged from 0.17 to 2,200 mg/L, and they were accordingly classified as follows: Class 2: n = 53; Class 3: n = 96; Class 4: n = 92; Class 5: n = 63; Class 6: n = 9, Class 7: n = 1; Class 8: n = 1 (there was no sample in Class 1). As classes 7 and 8 contained only one value, they were excluded from the validation process. For groundwater samples in each of the 5 retained salinity classes (2–6), the median of each chemical constituent was calculated (measured concentration) and correlated to the predicted concentrations presented in Table 2. The relationship between the measured and predicted concentrations in Figure 8 showed a strong correlation coefficient (R = 0.95; p-value <0.05 according to the Kendall statistical test). This high level of correlation indicates that the proposed predictive model was able to consistently predict the approximate concentrations, i.e., the chemical profile of all 12 of the studied chemical constituents.

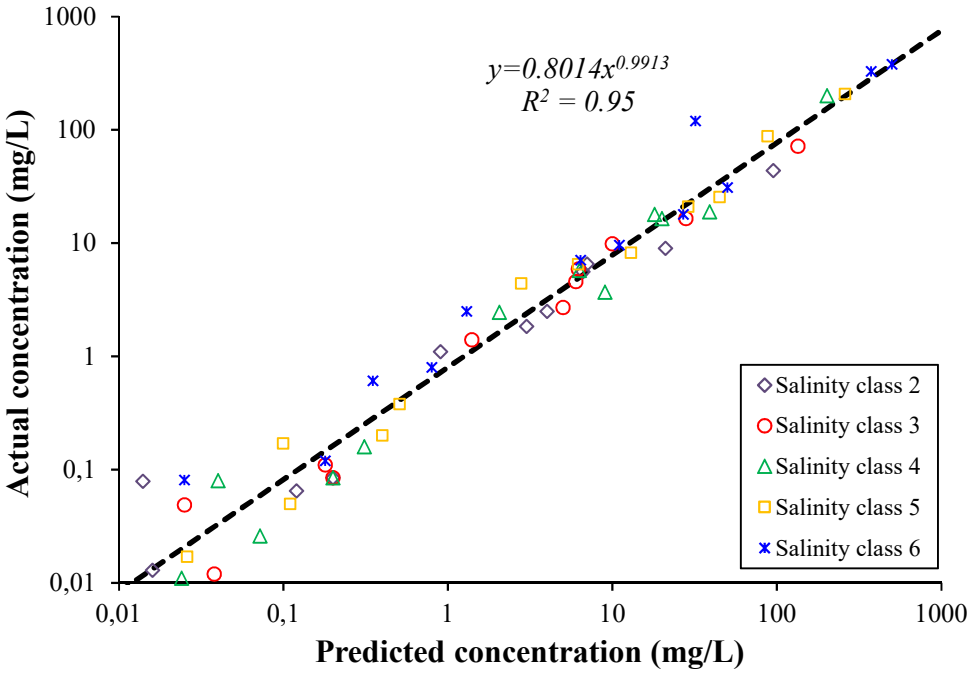

Fig. 8. Correlation between the predicted and measured concentrations (the 60 points in this figure represent 12 chemical constituents over 5 salinity classes of 313 groundwater samples).

6 DISCUSSION

Table 3 summarizes the distribution of dominant chemical elements within each salinity class. This table shows the transitions identified between the dominant chemical elements relative to Cl, as are the variable salinities at which major elements are dominant. In the present study, the distribution of chemical elements throughout the 8 salinity classes is further distinguished by comparing the dominant elements in the salinity classes using a Piper plot. Mg and K transitions are found in the moderate salinity classes 3 and 4, respectively (Table 3), but given the high Mg concentration over K concentration (10−15 times in meq/L), magnesium salt is dominant over potassium salt. However, Mg-Cl is not expected to be the dominant water type as the Piper diagram (Figure 9) shows that most groundwater samples from classes 6–8, with 25% of samples from class 5, are dominated by

Na-Cl water type, explained by the abundance of Na over Mg concentration. The transition, from Na dominant to Cl dominant groundwater, was observed over classes 3–7 (Table 3). The Piper plot (Figure 9) shows that samples from this transition distinguish two main water types. Here, 87% of samples from class 3 and 73% of samples from class 4 are overall dominated by a Ca-HCO_3 water type, whereas most samples from classes 6 (87%) and 7 (85%), as well as 25% from class 5, are generally dominated by a Na-Cl water type (Figure 9). The presence of a Ca-HCO_3 water type within this transition is related to the high concentration of Ca compared to Na in classes 3 and 4. In classes 5, 6 and 7, the dominance of Na concentration over Ca concentration explains the occurrence of a Na-Cl water type. Identifying class 5 as transition from HCO_3 and Ca dominant to Cl dominant appears to be logical, as the preceding classes 1–4 are dominated by a Ca-HCO_3 water type, whereas classes 6–8 are dominated by a Na-Cl water type (Figure 9).

Table 3. Distribution of dominant chemical elements in the 8 salinity classes.

	Salinity class							
	1	2	3	4	5	6	7	8
	Dominant water type* with % of groundwater samples							
	Ca-HCO3 (100%)	Ca-HCO3 (90%)	Ca-HCO3 (87%)	Ca-HCO3 (73%)	Ca-HCO3 (38%) Na-Cl (26%)	Na-Cl (87%)	Na-Cl (85%)	Na-Cl (100%)
Ca								
HCO_3								
K								
SO_4								
Mg								
Na								

Anion/cation-dominant Transition Cl-dominant

* Dominant water types are identified from Figure 7

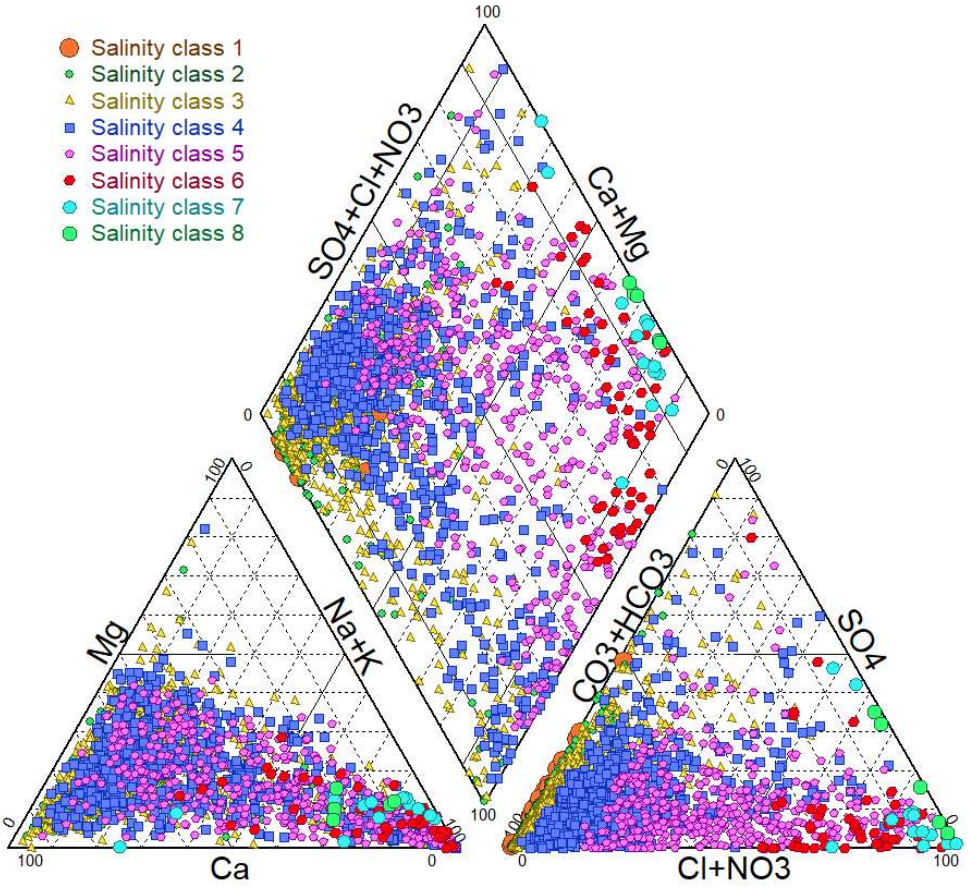

559

560 Fig. 9. Piper plot of groundwater samples by distinguishing their salinity classes.

561 An increase of the concentrations of the major elements (HCO_3, SO_4, Ca, Mg, Na, and K)
562 and some minor chemical constituents (Ba, B, and Sr) relative to the increase in Cl concentration is
563 observed in the PACES data. Similarly, Mora et al. (2020), who studied the dynamics of major and
564 trace elements along the groundwater flow path of the sedimentary Todos Santos aquifer in Baja
565 California Sur (Mexico), found that the major and minor elements exhibited increasing trends
566 relative to the increase in Cl concentration. The results from the present study —showing that major
567 elements, relative to the increase of Cl, were found to be dominant in the lower salinity classes,
568 whereas the Cl becomes dominant in the highest salinity classes— are also consistent with the

observations of Hanor (1994), who underlined that lower-salinity water often contains HCO_3 and SO_4 as dominant anions, whereas Cl makes up over 95% by mass of the anions in groundwater exhibiting a salinity greater than 10,000 mg/L. In the present study, as observed in the Todos Santos aquifer by Mora et al. (2020), the minor elements Si and F vary conservatively relative to the increase in Cl concentration. Cation exchange processes appeared to be responsible for the increase in Na and K relative to the increase in Cl concentrations in Todos Santos, whereas the increases in HCO_3, SO_4, and B were associated with the release of these elements due to carbonate mineral weathering (Mora et al. 2020). Numerous experimental studies have led to the understanding that certain geochemical processes govern the concentrations of chemical elements in groundwater relative to the increase in Cl concentration (Amrhein et al. 1992; Paalman et al. 1994; Sun et al. 2015). In the present study, the transition from Ca-dominant water to Cl-dominant water was observed at salinity class 5, i.e., in water that exhibits a Cl concentration of approximately 1.4−12.4 meq/L (10−50 mg/L). The decrease in Ca concentrations in salinity classes 5−6 suggests the involvement of high Cl concentration in causing the Ca-HCO_3-dominant groundwater to become Na-Cl-dominant groundwater (Moore et al. 2017). Such a process will lead to a decrease in Ca concentration. However, the high concentrations of Ca observed in classes 7−8, compared to the other salinity classes 1−6, can also result from incongruent weathering reactions (Wigley 1973). Like Ca, the other chemical constituents such as B, Ba, Sr, and Mg may also increase in concentration in groundwater during cation exchange (Charette and Sholkovitz 2006; Mahlknecht et al. 2017). Silica in groundwater is exclusively derived from water-rock interaction; the groundwater dissolves the silica through weathering of silicate minerals in rocks and sediments (Khan et al. 2015). The most common Si-bearing minerals are plagioclase, feldspars and quartz

591 (Miretzky and Alicia Fernàdez 2004). Analysis of cuttings from drilling wells in the study area
592 shows that silicate rocks (e.g., granite and gneiss) are rich in plagioclase-feldspar minerals
593 (Montcoudiol et al. 2015). This suggests initially that Si-groundwater in the study area may have
594 originated from the weathering of silicate rocks. However over the study area, Si concentrations in
595 groundwater were found to be limited to a maximum of 24 mg/L; this relatively low concentration
596 (1–30 mg/L) implies less water-rock interaction (Khan and Umar 2010). Silica can exist in solution
597 as chemically unreactive stable species, usually showing no affinity for other major dissolved
598 constituents (Haines and Lloyd 1985). This may explain why, through salinity classes 1−7 in the
599 present study, the median Si concentrations show a very slight variation ranging from 6 to 9 mg/L.
600 Strontium is a common trace element in most rocks and can be released into groundwater through
601 the weathering process as well as through the dissolution process, given its high solubility
602 (Middelburg et al. 1988; Moldovanyi et al. 1990; Luczaj and Masarik 2015). Strontium
603 concentrations are generally low in ultrabasic rocks and sandstones, but high concentrations have
604 been found in carbonate rocks (~600 ppm), evaporite media such as gypsum and anhydrite (~3,500
605 ppm), crystalline structures of feldspar plagioclase minerals and carbonate fossils (~10,000 ppm)
606 (Kinsman 1969; Beaucaire and Michard 1982; Franklyn et al. 1991). It is noteworthy that rocks of
607 the study area may contain high concentrations of Sr that contribute Sr to groundwater over all
608 salinity levels. Nonetheless, the observed increase in Sr concentration, relative to the increase of Cl,
609 is significantly higher than would be expected if weathering and/or dissolution processes were the
610 only sources of Sr. The increase in Sr relative to the increase in salinity may therefore also be linked
611 to other mechanisms occurring simultaneously. Sr can occur in combination with Ca and Ba
612 minerals, while Ba-rich groundwater generally contains significant concentrations of Sr (Bondu et

613 al. 2020). On the other hand, Sr can have several anthropogenic sources such as glass products (e.g.,
614 ceramics), fly ash from industrial waste coal burning, landfill leachate, and carbonate or phosphate
615 fertilizers (Musgrove 2021). Other geochemical processes such as sorption/desorption, co-
616 precipitation of minerals and mineral dissolution can also take place during the increase in salinity,
617 by involving an increasing/decreasing fraction of the concentrations in major, minor and trace
618 elements (Russak et al. 2016).

619 **7 CONCLUSION**

620 The present study provides a quantitative portrait of the variation in the concentrations of certain
621 chemical constituents in groundwater relative to the salinity level in Southern Quebec aquifers
622 (Canada). It also proposes a predictive model to determine the chemical profile of groundwater
623 based on the Cl concentration level. This study makes use of a groundwater chemistry database
624 containing data drawn from 2,608 groundwater samples from 16 Southern Quebec regions covering
625 a total surface area of approximately 100,000 km^2. The groundwater samples were collected from
626 private, municipal, and observation wells installed both in bedrock and unconsolidated aquifers.
627 This study considers 12 selected inorganic chemical constituents including major, minor, and trace
628 elements (i.e., HCO_3, SO_4, Ca, Mg, Na, K, Ba, B, Sr, Si, Mn and F). Based on the cumulative density
629 curve of Cl concentrations in the groundwater samples, eight salinity classes were established.
630 Graphical analyses were then applied to document the variations in the concentrations of these
631 chemical constituents throughout the established salinity classes. The results show that the
632 concentrations of chemical constituents increase as the Cl concentration increases; this finding is
633 consistent with those of other studies undertaken elsewhere under different contexts. On the other

hand, results show that the salinity of these groundwaters is largely controlled by Cl concentrations, although at low salinity, all of the major elements are important contributors. Concentrations of Ba, B and Sr increase with increasing Cl concentrations, whereas Si exhibits only limited increases in concentration with increasing salinity. The highest Mn and F concentrations are associated with the highest Cl concentrations. High concentrations of Mn and F, which in many cases exceed regulatory limits, constitute a serious issue in the management of drinking water quality in Southern Quebec's aquifers. Determining the origin of salinity over the study area is beyond the scope of the present study. However, given the observed increase of concentrations of chemical constituents relative to the increase of salinity, effective and sustainable groundwater resources management over the study area may depend on strategies that include the identification of the origins of groundwater salinity. Further studies investigating the sources of groundwater salinity at a regional scale are encouraged.

A predictive model of the major, minor and trace groundwater chemical constituents, relative to the Cl level, is proposed to help homeowners/groundwater managers gain valuable insight in regard to groundwater quality prior to costly laboratory analyses. The proposed predictive model was based on the 2009-2015 PACES groundwater chemistry data covering the regions of Southern Quebec, wherein the correlation between EC and Cl was identified as follows: $Cl = 0.0047 \times EC^{1.4273}$. The model could be further refined, and the uncertainty reduced by developing knowledge of the geochemical relationships within individual geologic regions, if necessary. The methodology established here for elaborating the predictive model in the present study could be adapted readily to other groundwater chemistry databases in other regions around the world. In the present study, an empirical predictive model of groundwater quality is proposed to determine the chemical profile of a groundwater by predicting the relative concentrations of a set of chemical constituents. This

study was limited to 12 inorganic chemical constituents, including some major elements as well as some minor and trace elements. However, it should be noted that a comprehensive prediction of groundwater quality would require the consideration of additional complementary chemical constituents of groundwater, in particular those that have severe adverse health effects. This study was based on the PACES groundwater chemistry database, which is comprised of data drawn from 2,608 groundwater samples collected in sixteen regions of Southern Quebec. The sixteen regions selected for PACES comprise the more densely inhabited regions of the province of Quebec. Consequently, complementary groundwater chemistry data drawn from other Southern Quebec regions would be valuable for future similar studies.

Acknowledgments

The authors would like to thank the Quebec Ministry of the Environment (*Ministère de l'Environnement et de la Lutte contre les Changements Climatiques*) that funded this project through the Groundwater Knowledge Acquisition Program (*Programme d'acquisition de connaissances sur les eaux souterraines - PACES*). The authors would like to thank two anonymous reviewers for their valuable comments and suggestions on improving this manuscript.

Statements & Declarations

Ethics approval: Not applicable

Consent to participate: Not applicable

Consent to publish: Not applicable

Author contributions: The first draft of the manuscript was written by Dr. Lamine Boumaiza and all authors **(**Julien Walter, Romain Chesnaux, Randy L. Stotler, Tao Wen, Karen H. Johannesson,

Karthikeyan Brindha, and Frédéric Huneau**)** commented on previous versions of the manuscript. All authors read and approved the final version of the manuscript.

Funding: This project is funded by the Quebec Ministry of the Environment (*Ministère de l'Environnement et de la Lutte contre les Changements Climatiques*) through the Groundwater Knowledge Acquisition Program (*Programme d'acquisition de connaissances sur les eaux souterraines - PACES*).

Competing interests: No potential conflict of interest was reported by the authors.

Availability of data and material: The data that supports the findings of the study are illustrated in the figures 2 to 6 of the present manuscript.

REFERENCES

Addinsoft (2021) XLSTAT statistical and data analysis solution. New York, USA. https ://www.xlsta t.com

Amrhein C, Strong JE, Mosher PA (1992) Effect of de-icing salts on metal and organic matter mobilization in roadside soils. Environ Sci Technol 26:703–709

ATSDR (Agency for Toxic Substances and Disease Registry) (2010) Toxicological Profile for Boron. Department of Health and Human Services, Public Health Service, Atlanta, GA: U.S.

Avrahamov N, Antler G, Yechieli Y, et al (2014) Anaerobic oxidation of methane by sulfate in hypersaline groundwater of the Dead Sea aquifer. Geobiology 12:511–528

Barbieri M, Ricolfi L, Vitale S, Muteto PV (2019) Assessment of groundwater quality in the buffer zone of Limpopo National Park, Gaza Province, Southern Mozambique. Environ Sci Pollut Res 26:62–77

Beaucaire C, Michard G (1982) Origin of dissolved minor elements (Li, Rb, Sr, Ba) in superficial waters in a granitic area. Appl Geochemistry 16:247–258

Beaudry C (2013) Hydrogéochimie de l'aquifèere rocheux régional en Montérégie est, Québec. Master's thesis, Université du Québec, Institut national de la recherche scientifique, Québec, Canada

Beaudry C, Lefebvre R, Rivard C, Cloutier V (2018) Conceptual model of regional groundwater flow based on hydrogeochemistry (Montérégie Est, Québec, Canada). Can Water Resour J 43:152–172

Benoit N, Nastev M, Blanchette D, Molson J (2014) Hydrogeology and hydrogeochemistry of the Chaudière River watershed aquifers, Québec, Canada. Can Water Resour J 39:32–48

Blanchette D, Lefebvre R, Nastev M, Cloutier V (2010) Groundwater quality, geochemical processes and groundwater evolution in the Chateauguay River watershed, Quebec, Canada.

711 Can Water Resour J 35:503–526
712 Bolduc AM, Ross M (2001) Géologie des formations superficielles, Lachute-Oka, Québec.
713 Geological Survey of Canada, Open File 3520; Natural Resources Canada
714 Bondu R, Cloutier V, Rosa E (2018) Occurrence of geogenic contaminants in private wells from a
715 crystalline bedrock aquifer in western Quebec, Canada: Geochemical sources and health risks.
716 J Hydrol 559:627–637
717 Bondu R, Cloutier V, Rosa E, Roy M (2020) An exploratory data analysis approach for assessing
718 the sources and distribution of naturally occurring contaminants (F, Ba, Mn, As) in
719 groundwater from southern Quebec (Canada). Appl Geochemistry 114:1–17
720 Boumaiza L, Chesnaux R, Drias T, et al (2020a) Identifying groundwater degradation sources in a
721 Mediterranean coastal area experiencing significant multi-origin stresses. Sci Total Environ
722 746:1–20
723 Boumaiza L, Chesnaux R, Walter J, Meghnefi F (2021a) Assessing response times of an alluvial
724 aquifer experiencing seasonally variable meteorological inputs. Groundw Sustain Dev 14:1–
725 12. https://doi.org/doi.org/10.1016/j.gsd.2021.100647
726 Boumaiza L, Chesnaux R, Walter J, Stumpp C (2020b) Constraining a flow model with field
727 measurements to assess water transit time through a vadose zone. Groundwater.
728 https://doi.org/doi.org/10.1111/gwat.13056
729 Boumaiza L, Chesnaux R, Walter J, Stumpp C (2020c) Assessing groundwater recharge and
730 transpiration in a humid northern region dominated by snowmelt using vadose-zone depth
731 profiles. Hydrogeol J 28:2315–2329
732 Boumaiza L, Chesnaux R, Walter J, Stumpp C (2021b) Numerical assessment of water transit-time
733 through a thick heterogeneous aquifer vadose-zone. In: Proceedings of the 74th Canadian
734 Geotechnical Conference and the 14th Joint CGS/IAH-CNC Groundwater Conference
735 (GeoNiagara-2021), Niagara Falls, Ontario, Canada. p 6
736 Boumaiza L, Rouleau A, Cousineau PA (2015) Estimation de la conductivité hydraulique et de la
737 porosité des lithofaciès identifiés dans les dépôts granulaires du paléodelta de la rivière Valin
738 dans la région du Saguenay au Québec. In: Proceedings of the 68th Canadian Geotechnical
739 Conference, Quebec City, Quebec, Canada. p 9
740 Boumaiza L, Rouleau A, Cousineau PA (2017) Determining hydrofacies in granular deposits of the
741 Valin River paleodelta in the Saguenay region of Quebec. In: Proceedings of the 70th Canadian
742 Geotechnical Conference and the 12th Joint CGS/IAH-CNC Groundwater Conference,
743 Ottawa, Ontario, Canada. p 8
744 Boumaiza L, Rouleau A, Cousineau PA (2019) Combining shallow hydrogeological
745 characterization with borehole data for determining hydrofacies in the Valin River paleodelta.
746 In: Proceedings of the 72nd Canadian Geotechnical Conference, St-John's, Newfoundland,
747 Canada. p 8
748 Boumaiza L, Walter J, Chesnaux R, et al (2021c) An operational methodology for determining
749 relevant DRASTIC factors and their relative weights in the assessment of aquifer vulnerability
750 to contamination. Environ Earth Sci 80:1–19. https://doi.org/doi.org/10.1007/s12665-021-
751 09575-w
752 Boumaiza L, Walter J, Chesnaux R, et al (2022) Groundwater recharge over the past 100 years:
753 regional spatiotemporal assessment and climate change impact over the Sauguenay-Lac-Saint-

754 Jean region, Canada. Hydrol Process 36:1–17. https://doi.org/doi.org/10.1002/hyp.14526
755 CEAEQ (Centre d'expertise en analyse environnementale du Québec) (2021) Méthodes d'analyses
756 CERM-PACES (2013) Résultats du programme d'acquisition de connaissances sur les eaux
757 souterraines de la région Saguenay-Lac-Saint-Jean. Centre d'études sur les ressources
758 minérales, Université du Québec à Chicoutimi
759 Chaillou G, Touchette M, Buffin-Bélanger T, et al (2018) Hydrogeochemical evolution and
760 groundwater mineralization of shallow aquifers in the Bas-Saint-Laurent region, Québec,
761 Canada. Can Water Resour J 43:136–151
762 Charette MA, Sholkovitz ER (2006) Trace element cycling in a subterranean estuary: part 2.
763 Geochemistry of the pore water. Geochim Cosmochim Acta 70:811–826
764 Chesnaux R (2013) Regional recharge assessment in the crystalline bedrock aquifer of the
765 Kenogami Uplands, Canada. Hydrol Sci J 58:421–436
766 Chesnaux R, Lambert M, Walter J, et al (2011) Building a geodatabase for mapping hydrogeological
767 features and 3D modeling of groundwater systems: Application to the Saguenay-Lac-St.-Jean
768 region, Canada. Comput Geosci 37:1870–1882
769 Chesnaux R, Stumpp C (2018) Advantages and challenges of using soil water isotopes to assess
770 groundwater recharge dominated by snowmelt at a field study located in Canada. Hydrol Sci J
771 63:679–695
772 Cloutier V, Lefebvre R, Savard MM, et al (2006) Hydrogeochemistry and groundwater origin of the
773 Basses-Laurentides sedimentary rock aquifer system, St. Lawrence Lowlands, Québec,
774 Canada. Hydrogeol J 14:573–590
775 Cloutier V, Lefebvre R, Savard MM, Therrien R (2010) Desalination of a sedimentary rock aquifer
776 system invaded by Pleistocene Champlain Sea water and processes controlling groundwater
777 geochemistry. Environ Earth Sci 59:977–994
778 Cloutier V, Lefebvre R, Therrien R, Savard MM (2008) Multivariate statistical analysis of
779 geochemical data as indicative of the hydrogeochemical evolution of groundwater in a
780 sedimentary rock aquifer system. J Hydrol 353:294–313
781 Cui Y, Wei M (2000) Ambient Groundwater Quality Monitoring and Assessment in BC: Current
782 Status and Future Directions. Groundwater Section, Ministry of Environment, Lands and
783 Parks, British Columbia, Canada
784 Deng YM, Wang YX, Ma T (2009) Isotope and minor element geochemistry of high arsenic
785 groundwater from Hangjinhouqi, the Hetao Plain, Inner Mongolia. Appl Geochemistry
786 24:587–599
787 Dessureault R (1975) Hydrogéologie du Lac Saint-Jean, partie nord-est. Ministère des richesses
788 naturelles du Québec, Direction générale des eaux, Service des eaux souterraines
789 Ding Y, Gao Y, Sun H, et al (2011) The relationships between low levels of urine fluoride on
790 children's intelligence, dental fluorosis in endemic fluorosis areas in Hulunbuir, Inner
791 Mongolia, China. J Hazard Mater 186:1942–1946
792 Elumalai V, Nwabisa DP, Rajmohan N (2019) Evaluation of high fluoride contaminated fractured
793 rock aquifer in South Africa geochemical and chemometric approaches. Chemosphere 235:1–
794 11
795 Evans AEV, Hanjra MA, Jiang Y, et al (2012) Water Quality: Assessment of the Current Situation
796 in Asia. Water Resour Dev 28:195–216

Ferroud A, Chesnaux R, Rafini S (2019) Drawdown log-derived analysis for interpreting constant-rate pumping tests in inclined substratum aquifers. Hydrogeol J 27:2279–2297
Ferroud A, Chesnaux R, Rafini S (2018) Insights on pumping well interpretation from flow dimension analysis: The learnings of a multi-context field database. J Hydrol 556:449–474
Foster SSD, Tuinhof A, Garduno H (2006) Groundwater development in Sub-Saharan Africa: a strategic overview of key issues and major needs. The World Bank GW-Mate Case Profile Collection no. 15, World Bank, Washington, DC
Franklyn MT, McNutt RH, Kamineni DC, et al (1991) Groundwater 87Sr/86Sr values in the Eye-Dashwa Lakes pluton, Canada: Evidence for plagioclase-water reaction. Chem Geol 86:111–122
Ghesquière O, Walter J, Chesnaux R, Rouleau A (2015) Scenarios of groundwater chemical evolution in a region of the Canadian Shield based on multivariate statistical analysis. J Hydrol Reg Stud 4:246–266
Government of Canada (2021) Canada's national climate archive. http://www.climate.weatheroffice.ec.gc.ca/climate_normals/ [consulted in July 2019]
Grassi S, Netti R (2000) Sea water intrusion and mercury pollution of some coastal aquifers in the province of Grosseto (Southern Tuscany - Italy). J Hydrol 237:198–211
Haines TS, Lloyd JW (1985) Controls on silica in groundwater environments in the United Kingdom. J Hydrol 81:277–295
Hamilton SM, Grasby SE, McIntosh JC, Osborn SG (2015) The effect of long-term regional pumping on hydrochemistry and dissolved gas content in an undeveloped shale-gas-bearing aquifer in southwestern Ontario, Canada. Hydrogeol J 23:719–739
Hanor JS (1994) Origin of saline fluids in sedimentary basins. Geol Soc London, Spec Publ 78:151–174
Health Canada (2020) Guidelines for Canadian Drinking Water Quality-Summary Table. Water and Air Quality Bureau, Healthy Environments and Consumer Safety Branch, Health Canada, Ottawa, Ontario, Canada
Hounslow AW (1995) Water quality data: Analysis and interpretation. Boca Raton, FL: Lewis
Howard KWF, Haynes J (1993) Groundwater contamination due to road de-icing chemicals — salt balance implications. Geosci Canada 20:1–8
Kendall MG (1975) Rank Correlation Method. Charless Griffin, London
Kennedy GW, Drage JM (2009) Hydrogeologic characterization of Nova Scotia's groundwater regions. In: The 62nd Canadian Geotechnical Conference and the 10th Joint CGS/IAH-CNC Groundwater Conference. IAH-CNC, Halifax, NS, Canada. pp 1230–1240
Khan A, Umar R, Khan HH (2015) Significance of silica in identifying the processes affecting groundwater chemistry in parts of Kali watershed, Central Ganga Plain, India. Appl Water Sci 5:65–72
Khan MMA, Umar R (2010) Significance of silica analysis in groundwater in parts of Central Ganga Plain, Uttar Pradesh, India. Curr Sci 98:1237–1240
Kinsman DJ (1969) Interpretation of Sr2+ concentrations in carbonate minerals and rocks. J Sediment Petrol 39:486–508
Koreimann C, Grath J, Winkler G, et al (1996) Groundwater monitoring in Europe. European Environment Agency Copenhagen, Denmark

840 Labrecque G, Chesnaux R, Boucher MA (2020) Water-table fluctuation method for assessing
841 aquifer recharge: application to Canadian aquifers and comparison with other methods.
842 Hydrogeol J 28:521–533
843 Ladevèze P, Rivard C, Lavoie D, et al (2019) Fault and natural fracture control on upward fluid
844 migration: insights from a shale gas play in the St. Lawrence Platform, Canada. Hydrogeol J
845 27:121–143
846 Lamothe M (1989) A New Framework for the Pleistocene Stratigraphy of the Central St. Lawrence
847 Lowland, Southern Quebec. Géographie Phys Quat 43:119–129
848 Lamothe M, St-Jacques G (2014) Géologie du Quaternaire des bassins versant des rivières Nicolet
849 et Saint-François, Québec. Ministère Énergies et Ressources Naturelles, Québec, Canada
850 Larocque M, Cloutier V, Levison J, Rosa E (2018) Results from the Quebec groundwater knowledge
851 acquisition program. Can Water Resour J 43:69–74
852 Lazur A, Van Derwerker T, Koepenick K (2020) Review of Implications of Road Salt Use on
853 Groundwater Quality-Corrosivity and Mobilization of Heavy Metals and Radionuclides. Water
854 Air Soil Pollut 231:1–10
855 Leahy PP, Thompson TH (1994) Overview of the National Water-Quality Assessment Program.
856 U.S. Geological Survey Open-File Report 94-70
857 Lefebvre R, Ballard JM, Carrier MA, et al (2015) Portrait des ressources en eau souterraine en
858 Chaudière-Appalaches, Québec, Canada. Projet réalisé conjointement par l'Institut national de
859 la recherche scientifique (INRS), l'Institut de recherche et développement en
860 agroenvironnement (IRDA) et le Regrou. Rapport final INRS R-1508, Ministère du
861 Développement durable, de l'Environnement et de la Lutte contre les changements climatiques,
862 Québec, Canada
863 Luczaj J, Masarik K (2015) Groundwater quantity and quality issues in a water-rich region:
864 examples from Wisconsin, USA. Resources 4:232–357
865 Mahlknecht J, Merchán D, Rosner M, et al (2017) Assessing seawater intrusion in an arid coastal
866 aquifer under high anthropogenic influence using major constituents, Sr and B isotopes in
867 groundwater. Sci Total Environ 587–588:282–295
868 Mann HB (1945) Nonparametric tests against trend. Econometrica 13:245–259
869 McCormack R, Therrien R (2013) St. Lawrence lowlands region. In: Alfonso, R. (Ed.), Canada's
870 Groundwater Resources. Fitzhenry & Whiteside. pp 501–539
871 Meinken W, Stober I (1997) Permeability distribution in the Quaternary of the Upper Rhine glacio-
872 fluvial aquifer. Terra Nov 9:113–116
873 MELCC (Ministère de l'Environnement et de la Lutte contre les changements climatiques) (2021)
874 Projets d'acquisition de connaissance des eaux souterraines.
875 https://www.environnement.gouv.qc.ca/eau/souterraines/programmes/acquisition-
876 connaissance.htm
877 Meriano M (2007) Groundwater-surface water interaction in Frenchman's bay watershed, Ontario:
878 Implications for urban recharge, contaminant storage and migration. Ph.D. Thesis, University
879 of Toronto, Canada
880 Meyzonnat G, Larocque M, Barbecot F, et al (2016) The potential of major ion chemistry to assess
881 groundwater vulnerability of a regional aquifer in southern Quebec (Canada). Environ Earth
882 Sci 75:1–12

883 Middelburg JJ, Van Der Weijden CH, Woittiez JRW (1988) Chemical processes affecting the
884 mobility of major, minor and trace elements during weathering of granitic rocks. Chem Geol
885 68:253–273
886 Minet EP, Goodhue R, Meier-Augenstein W, et al (2017) Combining stable isotopes with
887 contamination indicators: A method for improved investigation of nitrate sources and dynamics
888 in aquifers with mixed nitrogen inputs. Water Res 124:85–96
889 Miretzky P, Alicia Fernàdez C (2004) Silica dynamics in a pampean lake (Lake Chascomùs,
890 Argentina). Chem Geol 203:109–122
891 Moldovanyi E., Walter M, Brannon JC, Podosek FA (1990) New constraints on carbonate
892 diagenesis from integrated Sr and S isotopic and rare earth element data, Jurassic Smackover
893 Formation, U.S. Gulf Coast. Appl Geochemistry 5:449–470
894 Montcoudiol N, Molson J, Lemieux JM (2015) Groundwater geochemistry of the Outaouais Region
895 (Québec, Canada): a regional-scale study. Hydrogeol J 23:377–396
896 Moore J, Bird DL, Dobbis SK, Woodward G (2017) Nonpoint Source Contributions Drive Elevated
897 Major Ion and Dissolved Inorganic Carbon Concentrations in Urban Watersheds. Environ Sci
898 Technol Lett 4:198–204
899 Mora A, Mahlknecht J, Ledesma-Ruiz R, et al (2020) Dynamics of major and trace elements during
900 seawater intrusion in a coastal sedimentary aquifer impacted by anthropogenic activities. J
901 Contam Hydrol 323:1–17
902 Musgrove ML (2021) The occurrence and distribution of strontium in U.S. groundwater. Appl
903 Geochemistry 126:1–18
904 Nadeau S, Rosa E, Cloutier V (2018) Stratigraphic sequence map for groundwater assessment and
905 protection of unconsolidated aquifers: A case example in the Abitibi-Témiscamingue region,
906 Québec, Canada. Can Water Resour J 43:113–135
907 NBDE (New Brunswick Department of Environment) (2008) New Brunswick Groundwater
908 Chemistry Atlas: 1994-2007. Sciences and Reporting Branch, Sciences and Planning Division,
909 Environmental Reporting Series T2008-01
910 Oberhelman A, Peterson EW (2020) Chloride source delineation in an urban-agricultural watershed:
911 Deicing agents versus agricultural contributions. Hydrol Process 34:4017–4029
912 Paalman MAA, Van der Weijden CH, Loch JPG (1994) Sorption of cadmium on suspended matter
913 under estuarine conditions: competition and complexation with major seawater ions. Water Air
914 Soil Pollut 73:49–60
915 Pohlert T (2020) Non-Parametric Trend Tests and Change-Point Detection. https ://creat iveco
916 mmons .org/licen ses/by-nd/4.0/
917 Rango T, Vengosh A, Dwyer G, Bianchini G (2013) Mobilization of arsenic and other naturally
918 occurring contaminants in groundwater of the Main Ethiopian Rift aquifers. Water Res
919 47:5801–5818
920 Rey N, Rosa E, Cloutier V, Lefebvre R (2018) Using water stable isotopes for tracing surface and
921 groundwater flow systems in the Barlow-Ojibway Clay Belt, Quebec, Canada. Can Water
922 Resour J 43:173–194
923 Richard SK, Chesnaux R, Rouleau A, Coupe RH (2016) Estimating the reliability of aquifer
924 transmissivity values obtained from specific capacity tests: examples from the Saguenay-Lac-
925 Saint-Jean aquifers, Canada. Hydrol Sci J 61:173–185

926 Ricolfi L, Barbieri M, Muteto PV, et al (2020) Potential toxic elements in groundwater and their
927 health risk assessment in drinking water of Limpopo National Park, Gaza Province, Southern
928 Mozambique. Environ Geochem Health 42:2733–2745
929 Rouleau A, Clark ID, Bottomley DJ, Roy DW (2013) Precambrian Shield. In: Alfonso, R. (Ed.),
930 Canada's Groundwater Resources. Fitzhenry & Whiteside. pp 415–441
931 Rouleau A, Larocque M, Walter J, et al (2012) Le programme d'acquisition de connaissances sur
932 les eaux souterraines, Ses retombées dans les régions de Bécancour et du Saguenay–Lac-Saint-
933 Jean. Vecteur Environ 45:30–31
934 Russak A, Sivan O, Yechieli Y (2016) Trace elements (Li, B, Mn and Ba) as sensitive indicators
935 for salinization and freshening events in coastal aquifers. Chem Geol 441:35–46
936 Saby M, Larocque M, Pinti DL, et al (2016) Linking groudwater quality to residence times and
937 regional geology in the St. Lawrence Lowlands, southern Quebec, Canada. Appl Geochemistry
938 65:1–13
939 Santucci L, Carol E, Kruse E (2016) Identification of palaeo-seawater intrusion in groundwater
940 using minor ions in a semi-confined aquifer of the Rio de la Plata littoral (Argentina). Sci Total
941 Environ 566–567:1640–1648
942 Seddique AA, Masuda H, Anma R, et al (2019) Hydrogeochemical and isotopic signatures for the
943 identification of seawater intrusion in the paleobeach aquifer of Cox's Bazar city and its
944 surrounding area, south-east Bangladesh. Groundw Sustain Dev 9:1–12
945 Sun H, Alexander J, Gove B, Koch M (2015) Mobilization of arsenic, lead, and mercury under
946 conditions of sea water intrusion and road deicing salt application. J Contam Hydrol 180:12–
947 24
948 Swartz CH, Blute NK, Badruzzman B, et al (2004) Mobility of arsenic in a Bangladesh aquifer:
949 inferences from geochemical profiles, leaching data, and mineralogical characterization.
950 Geochim Cosmochim Actasmochim Acta 68:4539–4557
951 Thibaudeau P, Veillette J (2005) Géologie des formations en surface et histoire glaciaire.
952 Commission géologique du Canada, Lac Chicobi, Québec
953 Tremblay R, Walter J, Chesnaux R, Boumaiza L (2021) Investigating the potential role of geological
954 context on groundwater quality: a case study of the Grenville and St. Lawrence Platform
955 geological provinces in Quebec, Canada. Geosci 11:1–21
956 Vikas C, Kushwaha R, Ahmad W, et al (2013) Genesis and geochemistry of high fluorine-bearing
957 groundwater from a semi-arid terrain of NW India. Environ Earth Sci 68:289–305
958 Walter J (2018) Modèle d'évolution naturelle de l'eau souterraine dans une région du Bouclier
959 Canadien à partir de la détermination de pôles hydrogéochimiques régionaux. Ph.D Thesis,
960 Université du Québec à Chicoutimi, Québec, Canada
961 Walter J, Chesnaux R, Cloutier V, Gaboury D (2017) The influence of water/rock − water/clay
962 interactions and mixing in the salinization processes of groundwater. J Hydrol Reg Stud
963 13:168–188
964 Walter J, Chesnaux R, Gaboury D, Cloutier V (2019) Subsampling of regional-scale database for
965 improving multivariate analysis interpretation of groundwater chemical evolution and ion
966 sources. Geosci 9:1–32
967 Walter J, Rouleau A, Chesnaux R, et al (2018) Characterization of general and singular features of
968 major aquifer systems in the Saguenay-Lac-Saint-Jean region. Can Water Resour J 43:75–91

969 Wen T, Castro MC, Hall CM, et al (2015) Constraining groundwater flow in the glacial drift and
970 saginaw aquifers in the Michigan Basin through helium concentrations and isotopic ratios.
971 Geofluids 16:3–25
972 WHO (World Health Organization) (2017) Guidelines for drinking-water quality, 4th edition,
973 incorporating the 1st addendum. ISBN: 978-92-4-154995-0
974 Wigley T (1973) The incongruent solution of dolomite. Geochim Cosmochim Acta 37:1397–1402
975 Williams DD, Williams NE, Cao Y (2000) Road salt contamination of groundwater in a major
976 metropolitan area and development of a biological index to monitor its impact. Water Res
977 34:127–138
978 Yadav KK, Kumar V, Gupta N, et al (2019) Human health risk assessment: Study of a population
979 exposed to fluoride through groundwater of Agra city, India. Regul Toxicol Pharmacol
980 106:68–80
981 Yang JY, Wang M, Lu J, et al (2020) Fluorine in the environment in an endemic fluorosis area in
982 Southwest, China. Environ Res 184:1–10
983 Zango MS, Sunkari ED, Abu M, Lermi A (2019) Hydrogeochemical controls and human health risk
984 assessment of groundwater fluoride and boron in the semiarid North East region of Ghana. J
985 Geochemical Explor 207:1–21
986 Zendehbad M, Cepuder P, Loiskandl W, Stumpp C (2019) Source identification of nitrate
987 contamination in the urban aquifer of Mashhad, Iran. J Hydrol Reg Stud 25:1–14
988
989
990